On the Difference in Deformation Behaviour between Phenocryst and Ground-mass Quartz of Deformed Rhyolite Pebbles in the Oboke Conglomerate Schist

By

Ikuo HARA, Yûjiro NISHIMURA and Tsugio ISAI

with 6 Tables, 51 Text-figures and 4 Plates

(Received April 30, 1966)

ABSTRACT: Quartz subfabrics of the conglomerate schist consisting of rhyolite pebbles and psammitic matrix of the Oboke district, Shikoku, Southwest Japan, have been described and discussed in detail, with special reference to deformation mechanisms of quartz taking place under metamorphic conditions. Quartz grains in the deformed rhyolite pebbles and the psammitic matrix occur generally in two distinctly separated sizes, that is, porphyritic grains of phenocryst quartz in rhyolite and clastic megacryst in psammitic matrix, and fine-grained quartz smaller than one tenth of the former in size, derived from glassy or cryptocrystalline material of the ground-mass of rhyolite and from very fine-grained material of psammitic matrix. The fine-grained quartz grains, except for those surrounding the porphyritic quartz grains, show clearly preferred lattice and dimensional orientation in such a fashion as are symmetrically consistent with the mesoscopic structures of the conglomerate schist of the district. The patterns of lattice and dimensional subfabrics of the fine-grained quartz are essentially the same as those of calcite in the rhyolite pebbles, and the former is symmetrically consistent with the latter. While, for the porphyritic quartz in the rhyolite pebbles and psammitic matrix no preferred lattice orientation has been recognized. The pattern of dimensional orientation of those grains is quite different from that of the fine-grained quartz. The significance of difference in pattern of lattice and dimensional subfabrics between the fine-grained quartz and the porphyritic quartz has been discussed. It is assumed that, when metamorphic deformation induced preferred lattice and dimensional orientations to the fine-grained quartz, deformation of the porphyritic quartz occurred by translation gliding on a certain crystallographic plane, accompanied with the formation of kink bands and recrystallization in those bands and grain-boundaries, though no preferred lattice and dimensional orientations were induced to those coarse-grained quartz grains. Obtained data inclines our mind to such a view that for the deformation of quartz taking place under metamorphic conditions diffusion mechanisms, including nucleation, grain-boundary migration and Riecke diffusion, play the more predominant role than translation gliding on some particular crystallographic planes does. In the Sambagawa crystalline schists of the higher metamorphic grade (e.g., the zone IV in the Kôtsu-Bizan district after Iwasaki, 1963) than that for those of the Oboke district (corresponding to the zone II in the Kôtsu-Bizan district), quartz grains with the average size, which is nearly equal to that of the porphyritic quartz grains in question (no preferred lattice orientation), show a preferred lattice orientation, whose pattern is essentially the same as that of the c-axis subfabric of the fine-grained quartz in question. The average size of quartz grains, which show preferred lattice orientation, increases with increase in the metamophic grade, giving an equilibrium size under any metamorphic deformation condition.

CONTENTS

I. INTRODUCTION

Since the summer of 1964, the authors have examined the quartz subfabric of the conglomerate schist, consisting of rhyolite pebbles and psammitic matrix, of the Oboke district, Shikoku, Southwest Japan. Preliminary study of the deformed rhyolite pebble indicated marked differnce in pattern of the lattice subfabric between coarse-grained quartz, originally quartz phenocryst, and fine-grained quartz, generally smaller than one tenth of the former in size, derived from glassy or cryptocrystalline ground-mass of rhyolite. The former shows no preferred lattice orientaition, while the latter shows definitie pattern of lattice orientation, which is symmetrically consistent with mesoscopic fabrics of the conglomerate schist. In order to assess more accurately the difference in question, detailed statistical studies of both lattice and dimensional subfabrics of quartz in the rhyolite pebbles and psammitic matrix have been undertaken. In this paper will be described and discussed the results obtained, with special reference to the deformation mechanism of quartz taking place under the physical condition where metamorphism occurs.

Acknowledgements: The authors are especially indebted to Prof. G. KOJIMA for his critical review of the manuscript. The field work for this study was supported in part by the Grant in Aid for Scientific Researches from the Ministry of Education.

II. GEOLOGICAL SETTING

The conglomerate schist in question belongs stratigraphically to the lower formation, the Oboke formation, of the crystalline schist system of the Sambagawa metamorphic belt in Shikoku (KOJIMA, 1951; KOJIMA, HIDE and YOSHINO, 1956). It is impossible to estimate the total thickness of the sediments overlain on the conglomerate schist of the Oboke district at the time of the Sambagawa metamorphic deformation. KOJIMA (1958) estimated the total thickness of the Sambagawa schist formations to attain 5,320 to 11,460 m.

The metamorphism of the Sambagawa belt in Shikoku belongs to the high-pressure intermediate group of the metamorphic facies series (or the glaucophanitic metamorphism) after MIYASHIRO (1965). The metamorphic grade of the conglomerate schist of the Oboke district corresponds to that of the zone II of the Kôtsu-Bizan district, east of Oboke, studied by IWASAKI (1963), according to his personal communication (1965). Psammitic schist, including the conglomerate schist of the Oboke district, was studied petrographically by KOJIMA and MITSUNO (1950). They found such kinds of relict clastic minerals as orthoclase, microcline, augite, brown or green common hornblend, tourmaline (brownish), garnet, allanite, epidote, titanite, and zircon.

The geologic structure of the Oboke district is characterized by an anticline, the Oboke anticline in Fig. 1. The conglomerate schist is distributed at the crest and

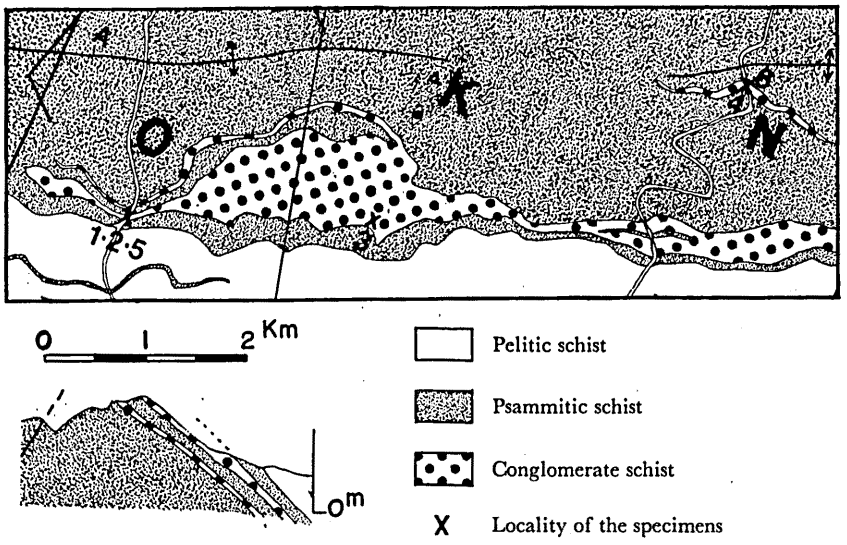

FIG. 1 Geological map of the Oboke district after KOJIMA and MITSUNO (1966).
O: Oboke K: Kunimi-yama N: Nemuri-dani
1, 2, 3, 4, 5 and 6: Localities of the specimens I, II, III, IV, V and VI, respectively, of the rhyolite pebbles and psammitic matrix, whose calcite and quartz subfabrics have been examined.
A: Axis of the Oboke anticline.

the southern limb of the anticline.

The structure of the conglomerate schist and surrounding psammitic schist is generally characterized by two types of planar structure and a linear structure. One of the planar structures is schistosity (here termed S_1), defined by preferred orientation of flaky minerals, which is parallel to the bedding surface and the other is strain-slip cleavage in the sense of KNILL (1960), (here termed S_2), which traverses the schistosity surface at high angles, —— the S_2-cleavage includes the S_2-cleavage and S_3-cleavage by NAKAGAWA (1965). The linear structure (here termed L_{1-2}) is displayed as the line of intersection of the S_1-schistosity and S_2-cleavage. The S_2-cleavage is roughly parallel to the axial plane of the anticline, and the L_{1-2}-lineation is parallel to its axis (NAKAGAWA, 1965). Generally, deformed pebbles of the conglomerate schist show remarkable lensoid form elongated parallel to the S_1-schistosity (Plate 7-1). The S_2-cleavage is much less developed in the deformed pebbles than in the psammitic matrix.

On the basis of analysis of mesoscopic structures, the tectonic history of the Sambagawa crystalline schists of the Oboke district can be illustrated in the order of younging as follows: 1) the deformation related to S_1-schistosity and to the formation of marked lensoid form of pebbles in the conglomerate schist, which are preferably elongated parallel to the S_1-surface, (here termed the S_1-deformation). 2) the deformation related to the S_2-cleavage (here termed the S_2-deformation). And 3)

jointing and faulting.

III. Analysis of Calcite and Quartz Subfabrics of the Oboke Conglomerate Schist

A. General Statement

Calcite and quartz subfabrics have been studied on three mutually perpendicular thin sections cut from four specimens of rhyolite pebbles and from two specimens of psammitic matrix (only quartz subfabrics). Of these thin sections, the first is cut perpendicular to the L_{1-2}-lineation (ac-section), the second parallel to L_{1-2} and perpendicular to S_1 (bc-section), and the third parallel to S_1 (ab-section). The localities of the six specimens of the conglomerate schist are shown in Fig. 1.

The rhyolite pebbles examined consist mainly of quartz, plagioclase, calcite, white mica, chlorite and pumpellyite, among which quartz is the most abundance. It is rather easy to distinguish original phenocrysts from original ground-mass. In the ground-mass, however, grains of quartz, calcite, white mica and pumpellyite do not occure as a mixture, but they tend to form pools or bands of respective mineral species. Quartz-rich pools and bands are commonly found, in which quartz attains to more than 90 per cent. For convenience' sake, quartz grains in those pools or bands of the ground-mass are named Q_{rg} (Plate 7–2). Quartz is the most abundant one of minerals porphyritically developed in the rhyolite pebbles. In quartz phenocrysts (here termed Q_{rc}) are commonly developed clearly defined small subgrains (here termed Q_{rs}) (Plate 9–1 and 2). It is interesting that pressure-shadow-like fine-grained feather quartzs (here termed Q_{rf}) and white mica are frequently developed around quartz phenocrysts (Plate 8–2).

The psammitic matrix consists chiefly of quartz, plagioclase and white mica. Quartz of the psammitic matrix can be grouped roughly into two groups after its grain-size, that is, coarse-grained quartz which is originally coarse-grained clastic quartz, and fine-grained quartz, probably derived from the very fine-grained materials of the ground-mass. The quartz grains of the former type will be named Q_{sc}, and those of the latter type Q_{sg}. Around the Q_{sc}-grains are commonly found pressure-shadow-like feather quartzs (here termed Q_{sf}) and white mica (Plate 8–1). In the Q_{sc}-grains clealy defined small subgrains (here termed Q_{ss}) are commonly developed.

In the conglomerate schist quartz veins are frequently found. They are classified into two types after microscopic features, that is, the first type consists of fine-graind subgrains (here termed Q_{vs}) derived from the coarse-grained vein-quartz (Plate 9–3), and the second type consists of quartz grains without granulation texture.

Symboles	Materials
Q_{rc}	Coarse-grained quartz porphyritically developed in rhyolite pebbles, originally phenocryst quartz.
Q_{rg}	Fine-grained quartz in quartz-rich pools of the ground-mass of rhyolite pebbles, derived from the very fine-grained materials of the ground-mass by recrystallization.
Q_{rs}	Clearly defined small subgrains in Q_{rc}-grains.
Q_{rf}	Feather quartz in pressure-shadows around Q_{rc}-grains.
Q_{sc}	Coarse-grained quartz porphyritically developed in psammitic matrix, originally coarse-grained clastic quartz.
Q_{sg}	Fine-grained quartz in psammitic matrix, derived from the very fine-grained materials of the ground-mass by recrystallization.
Q_{ss}	Clearly defined small subgrains in Q_{sc}-grains.
Q_{sf}	Feather quartz in pressure-shadows around Q_{sc}-grains.
Q_{vs}	Clearly defined small subgrains in coarse-grained vein-quartz.

B. Calcite Subfabrics of Rhyolite Pebbles

1) *Distribution of apparent grain size of calcite.*

Method of estimating real size of grain in crystalline aggregate based on microscopic examination of a plane section has been discussed by many authors (e.g., Scheil, 1935; Rutherford, Aborn and Bain, 1937; Galwey and Jones, 1963). However, these methods will not be used in estimating the grain size of calcite and quartz in the rhyolite pebbles and psammitic matrix. In this paper will be described only distribution of the apparent size of calcite and quartz observed on the ac-section, that is, the diameter of cross-sectional area of individual grains. The apparent grain size X for each grain is given by the following equation $X=\sqrt{AB}$, when A is the length of grain in the direction of the least projection and B is the length of grain in the direction perpendicular to the former.

Fig. 2 shows the distribution of the apparent size of 200 calcite grains observed on the ac-sections, 50 from each of four ac-sections cut from four specimens of rhyo-

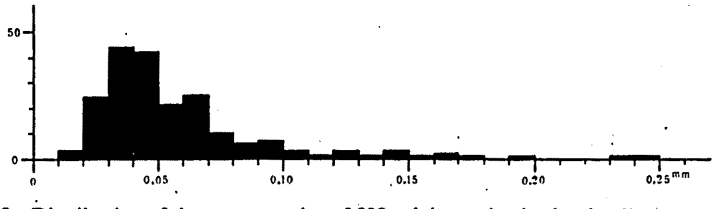

Fig. 2 Distribution of the apparent size of 200 calcite grains in the rhyolite pebbles as measured on the ac-sections. The frequency is given by the number of grains.

lite pebbles (specimens I, II, III and IV). The apparent size of calcite grain is between 0.02 mm and 0.25 mm, with single maximum between 0.04 mm and 0.05 mm.

2) *Dimensional orientation of calcite*

In order to define the orientation of calcite and quartz grains on the section, the following method of analysis is used in this paper. The orientation of each grain is measured as the direction in which the two most closely spaced parallel lines can be drawn tangent to the outline of the grain. Grains are measured without selection; in each section all the grains in a series of fields of view were measured until a total of 50 was reached. As a means of statistical expression of the direction and the degree of preferred orientation of the grains, a simple two-dimensional scheme of vector analysis is employed, according to CURRAY (1959). As the final criterion for the significance of preferred orientation, the Rayleigh test of significance (CURRAY, 1956) is adopted. No distribution is accepted as being significantly different from uniformity, unless the probability is less than 0.05.

The results are shown in Tables 1 to 4. On the ac-section and bc-section of the specimen IV, the direction of preferred dimensional orientation (vector mean) is approximately parallel to the trace of the S_1-surface, that is, the direction of elongation of lensoid rhyolite pebbles. While, on the ab-section for the specimen IV, the direction of vector mean is approximately parallel to the L_{1-2}-lineation. Therefore, it can be inferred that most calcite grains in the rhyolite pebble of the specimen IV tend to orient with the longest axis in the direction parallel to the L_{1-2}-lineation, the intermediate axis in the direction parallel to the S_1-surface and perpendicular to the L_{1-2}-lineation, and the shortest axis in the direction perpendicular to the S_1-surface. Unfortunately, on the bc-sections of the specimens I and II and on the ab-sections of the specimens II and III, the numbers of calcite grains are too small to determine statistically their dimensional orientation. On the bc-section of the specimen III, the direction of preferred dimensional orientation of calcite is approximately parallel to the trace of S_1-surface, like in the case of the specimen IV. On the ab-section of the specimen I, the direction of vector mean is approximatelly parallel to the L_{1-2}-lineation, like in the case of the specimen IV. The pattern of the dimensional subfabrics of calcite grains of the specimens I, II and III may be similar to that of the specimen IV.

3) *c-axis subfabric of calcite*

The c-axis subfabric diagrams for calcite in the rhyolite pebbles are shown in Figs. 3 to 6. Each diagram is based on 200 calcite c-axes measured on the ac-section for each of four rhyolite pebbles. All the diagrams show a distinct cleft-girdle with maxima and submaxima on a small circle at ca. 60° to 75° to the girdle axis. In Fig. 4 (the specimen II) the girdle is broken near the direction of vector mean for the calcite dimensional orientation, subparallel to the trace of S_1-surface, on the ac-section. The girdle axis coincides with the direction of grain elongation statistically determined in the previous section and with the L_{1-2}-lineation.

Analogous pattern of calcite c-axis fabric was interpreted in terms of stress by

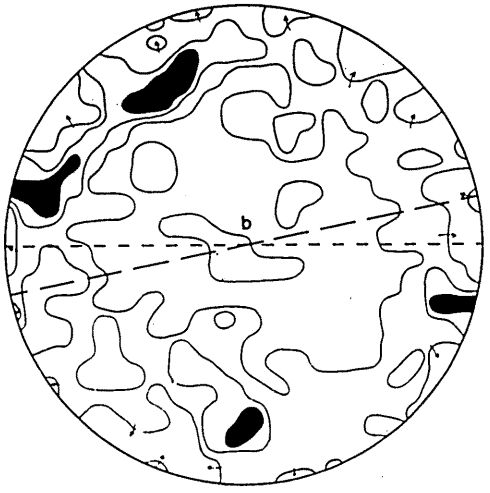

FIG. 3 The c-axis subfabric of 200 calcite grains in the rhyolite pebble (specimen I). Contours: 3-2-1 %. b: the direction of the L_{1-2}-lineation. dash line: the S_1-surface. broken line: the direction of vector mean.

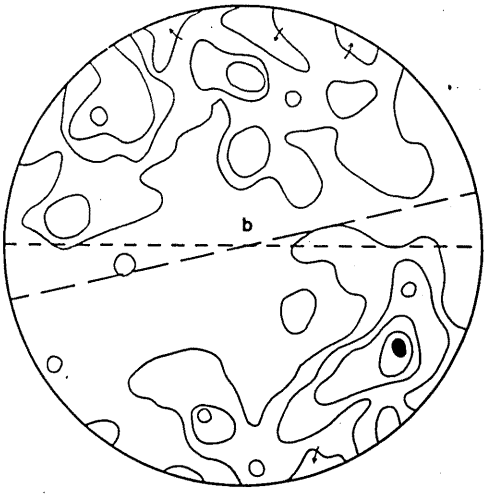

FIG. 4 The c-axis subfabric of 200 calcite grains in the rhyolite pebble (specimen II). Contours: 5-4-3-2-1 %.

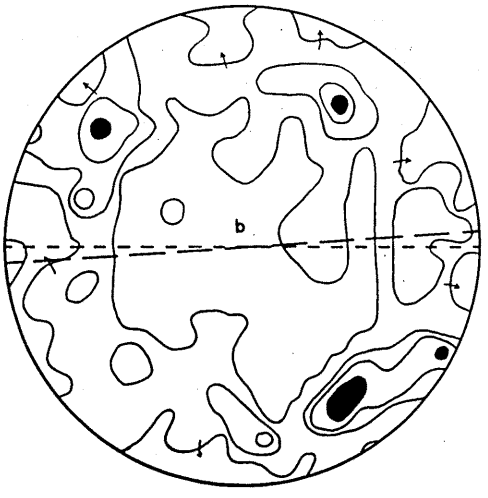

FIG. 5 The c-axis subfabric of 200 calcite grains in the rhyolite pebble (specimen III). Contours: 4-3-2-1 %.

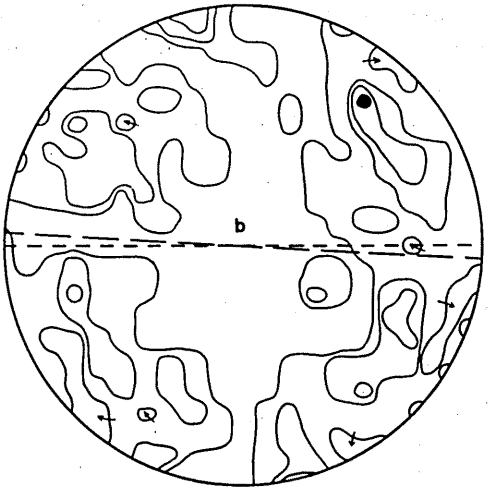

FIG. 6 The c-axis subfabric of 200 caicite grains in the rhyolite pebble (specimen IV). Contours: 4-3-2-1 %.

TURNER *et al.* (1963) on the basis of experimental evidences: "a cleft-girdle pattern of c-axes, with maxima on a small circle at 60° to 70° to the girdle axis (=direction of grain elongation) is consistent with axially symmetric extension parallel to the axis of minimal principal stress. This corresponds to what SANDER has called Ein-

engung…." (p.413). This interpretation may also be valid for the calcite subfabric of the rhyolite pebbles in question. It is assumed on the basis of experimental evidences (TURNER and CH'IH, 1951; TURNER, GRIGGS, CLARK and DIXON, 1956; GRIGGS, TURNER, and HEARD, 1960; HEARD, 1963; FERREIRA and TURNER, 1964) that the pattern of calcite c-axis fabric, for which syntectonic recrystallization is responsible, is different from that produced by direct componental movement such as translation gliding and twin gliding. For the calcite subfabrics of the rhyolite pebbles, it can be pointed out that the orienting process of the latter type played the predominant role.

C. QUARTZ SUBFABRICS OF RHYOLITE PEBBLES

1) *c-axis subfabric of quartz*

a) c-axis subfabric for quartz phenocrysts (Q_{rc}): The c-axis subfabric diagrams for Q_{rc}-grains (Figs. 7 to 10) of rhyolite pebbles (the specimens I, II, III and IV) are based on the measurment of 200 axes on each ac-section. It appears that no preferred orientation is shown in the diagram.

b) c-axis subfabric for quartz in quartz-rich pools of the ground-mass (Q_{rg}): The c-axis subfabric diagrams for Q_{rg}-grains are given in Figs. 11 to 16, showing marked preferred orientation, unlike the case of Q_{rc}-grains. Figs. 11, 13, 14, 15 and 16 are respectively based on the measurment of 200 c-axes on each of the ac-sections cut from the specimens I, II, III and IV, while Fig. 12 is based on 200 axes measured on the ab-section of the specimen I. Figs. 15 and 16 show the c-axis subfabric for Q_{rg}-grains in separate pools in the pebble of the specimen IV.

As is obvious in Figs. 11 to 14, the pattern of the fabric diagrams for Q_{rg}-grains

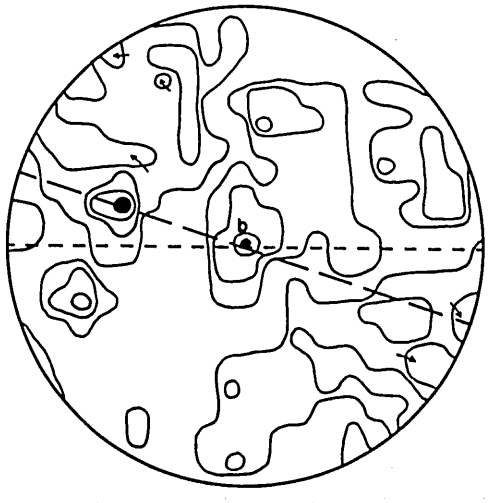

FIG. 7 The c-axis subfabric of 200 Q_{rc}-grains in the rhyolite pebble (specimen I). Contours: 4-3-2-1 %.

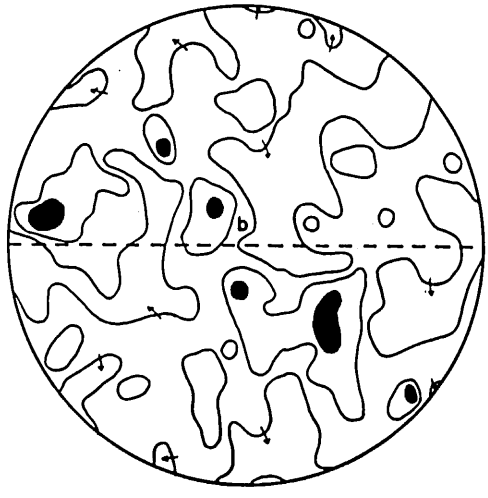

FIG. 8 The c-axis subfabric of 200 Q_{rc}-grains in the rhyolite pebble (specimen II). Contours: 3-2-1 %.

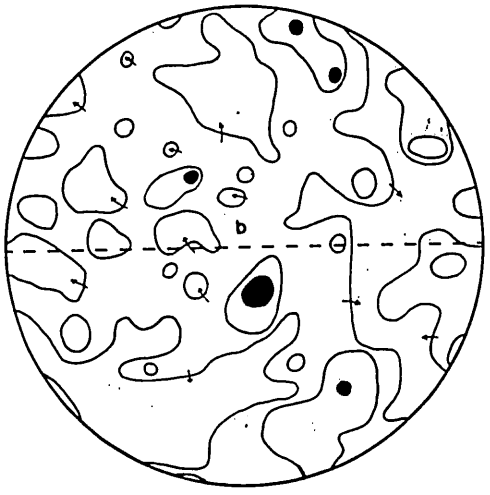

FIG. 9 The c-axis subfabric of 200 Q_{rc}-grains in the rhyolite pebble (specimen III). Contours: 3-2-1 %.

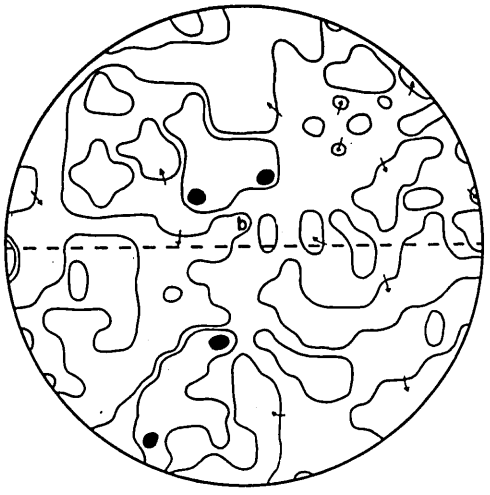

FIG. 10 The c-axis subfabric of 200 Q_{rc}-grains in the rhyolite pebble (specimen IV). Contours: 3-2-1 %.

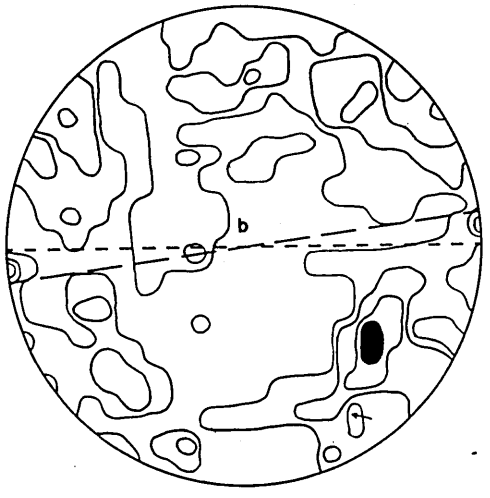

FIG. 11 The c-axis subfabric of 200 Q_{rg}-grains in the rhyolite pebble (specimen I). Contours: 4-3-2-1 %.

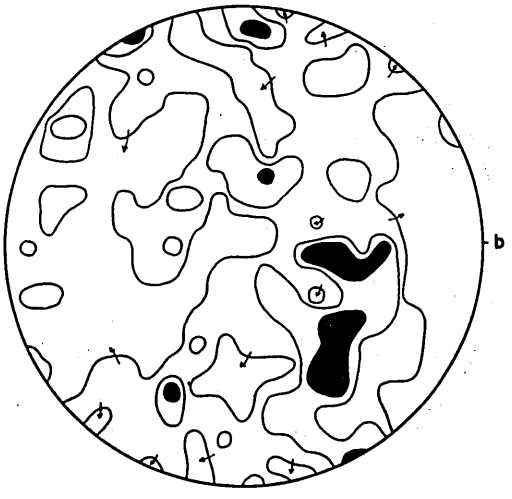

FIG. 12 The c-axis subfabric of 200 Q_{rg}-grains in the rhyolite pebble (ab-section cut from the specimen I). Contours: 3-2-1 %.

in the specimens I, II and III is characterized by a distinct cleft-girdle with maxima and submaxima on a small circle at 60° to the girdle axis, though, in Fig. 13 (for the specimen II), the girdle is clearly broken near the direction parallel to the trace of the S_1-surface on the ac-section. The girdle axis coincides with the L_{1-2}-lineation and with the direction of grain elongation, which will be statistically examined

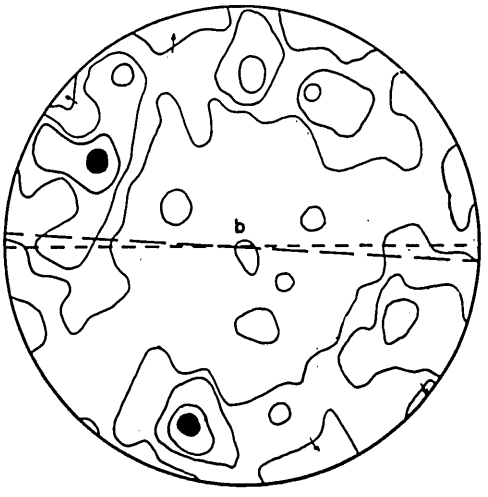

FIG. 13 The c-axis subfabric of 200 Q_{rg}-grains in the rhyolite pebble (specimen II). Contours: 4-3-2-1 %.

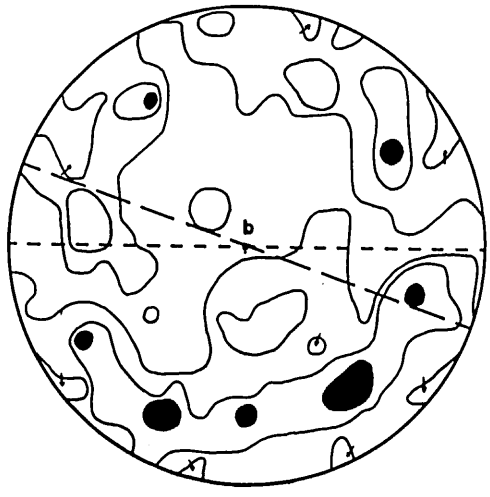

FIG. 14 The c-axis subfabric of 200 Q_{rg}-grains in the rhyolite pebble (specimen III). Contours: 3-2-1 %.

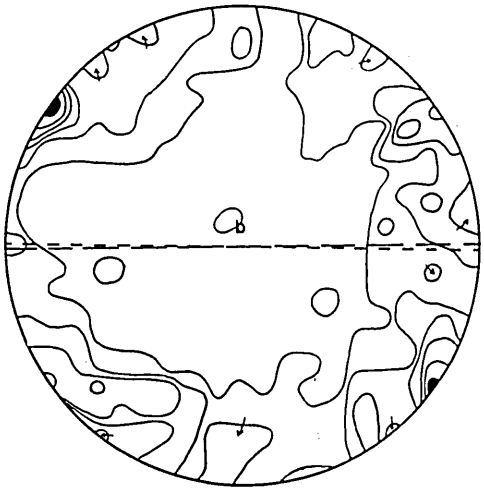

FIG. 15 The c-axis subfabric of 200 Q_{rg}-grains in the rhyolite pebble (specimen IV). Contours: 6-5-4-3-2-1 %.

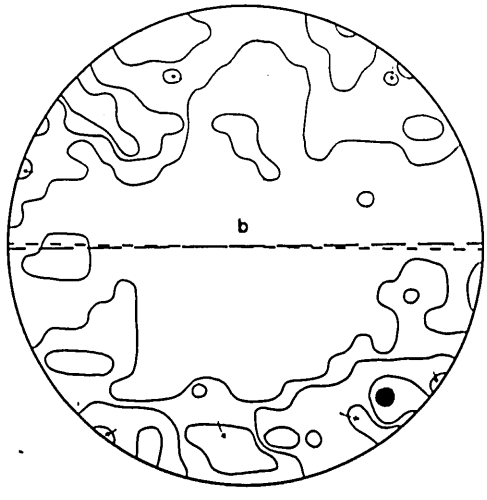

FIG. 16 The c-axis subfabric of 200 Q_{rg}-grains in the rhyolite pebble (specimen IV). Contours: 4-3-2-1 %.

in the following pages. The cleft-girdle pattern of c-axes for Q_{rg}-grains in the specimens I, II and III is quite similar to that for calcite grains described in the preceding pages, as is obvious when Figs. 11, 13 and 14 are compared with Figs. 3, 4 and 5, respectively.

Figs. 15 and 16 for the specimen IV are characterized by a great circle girdle with maxima and submaxima, unlike the cases of Figs. 11 to 14 for the specimens I,

II and III. The girdle axis coincides with the L_{1-2}-lineation and with the direction of grain elongation. In the specimen IV, the fabric pattern for Q_{rg}-grains (a great circle girdle) is different from that for calcite grains (a small circle girdle), unlike the cases of the specimens I, II and III.

It has been shown that for the lattice and dimensional subfabrics of calcite and quartz in the rhyolite pebbles the symmetry axis (=the girdle axis=the direction of grain elongation) coincides with that of the mesoscopic rock structure (=the L_{1-2}-

FIGS. 17 to 30 The c-axis subfabric of Q_{rs}-grains which show the mode of occurrence of the first type. crosses: the c-axis of host Q_{rc}-grain. Solid straight line: the trend of band on the plane of ac-section.

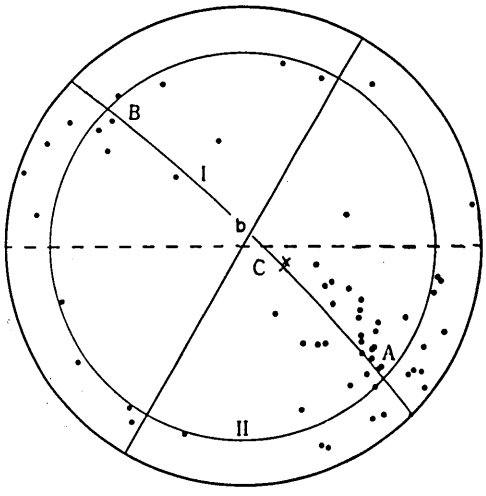

FIG. 17

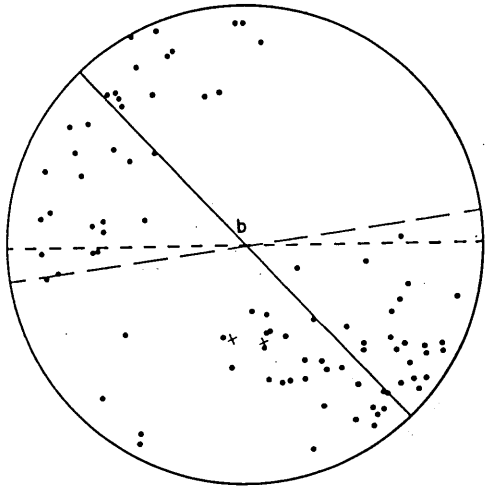

FIG. 18

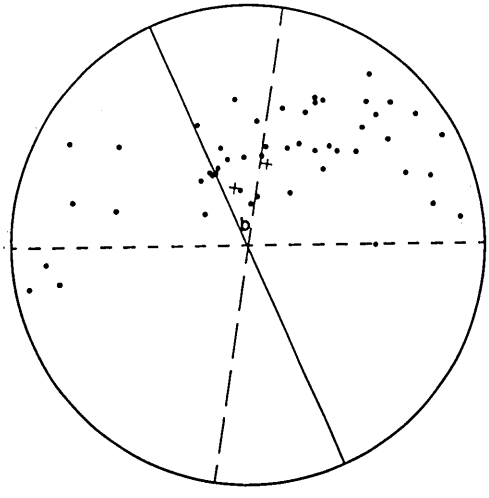

FIG. 19

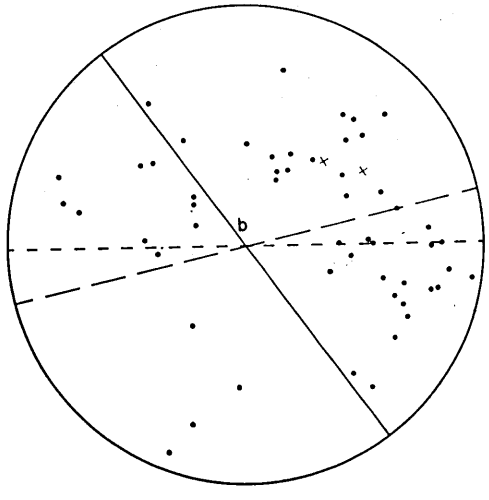

FIG. 20

lineation). According to the symmetry principle elaborated by SANDER (1948) and PATERSON and WEISS (1961), it can be assumed that the lattice and dimensional subfabrics of calcite grains and Q_{rg}-grains in question are related to the deformation responsible for the formation of mesoscopic rock structures (S_1 and S_2) as well as of major structure (Oboke anticline).

c) c-axis subfabric for subgrains in quartz phenocrysts (Q_{rs}): The mode of occurrence of subgrains in quartz phenocrysts of rhyolite pebbles can be divided into two types: In the first type, subgrains occur in a band, straightly traversing the phenocryst (Q_{rc}) and terminating within the grain-boundaries, (Plate, 9-1), and in the second type, subgrains occur in marginal to internal parts of the phenocryst, showing no band structure (Plate 9-2).

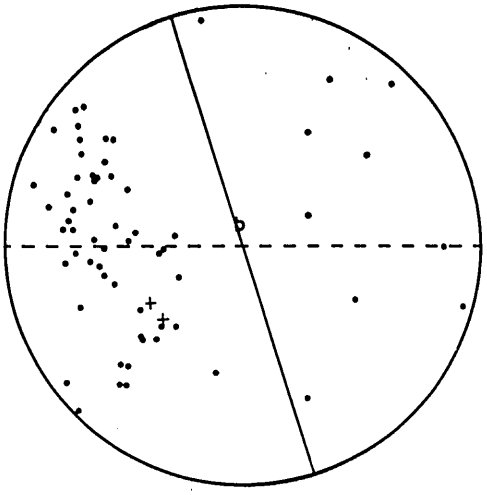

FIG. 21

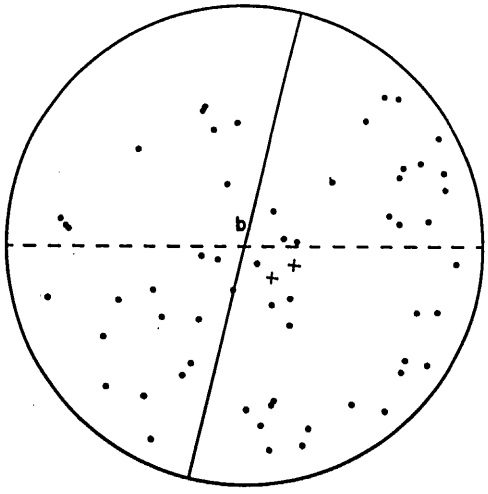

FIG. 22

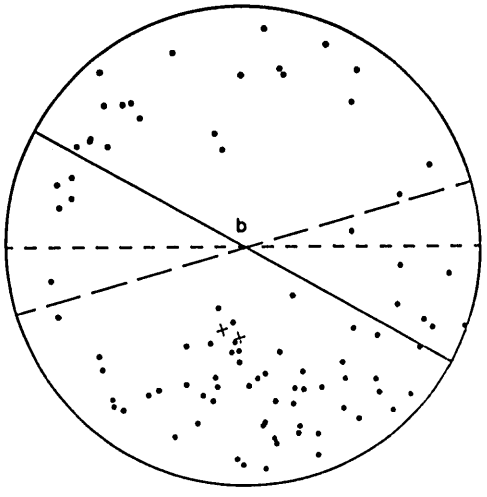

FIG. 23

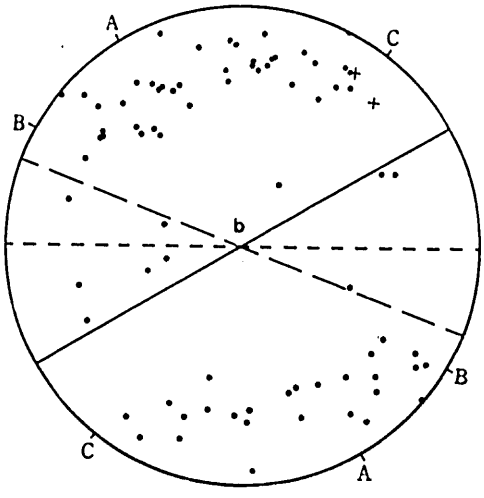

FIG. 24

The characteristic features of the c-axis subfabric for the subgrains of the first type, shown in Fig. 17, are enumerated as follows: 1) The c-axes are distributed on two girdles, that is, girdle I and girdle II in Fig. 17. The great circle girdle I comprises the c-axis of the host crystal. While the small circle girdle II lies at ca. 70° to the L_{1-2}-lineation. 2) The girdle I is incomplete, and most c-axes are distributed on this girdle from the point C (the c-axis of the host grain), through A, to B, and between C and B the girdle is completely broken. Similar patterns have been obtained for the subgrains of the first type in other quartz phenocrysts, whose c-axis lie at low to moderate angles to the L_{1-2}-lineation (Figs. 17 to 23). It can be noticed that, in these figures, the concentration of c-axes on the girdle I is quite asymmetric across the projection point of the c-axis of the host grain, showing a ten-

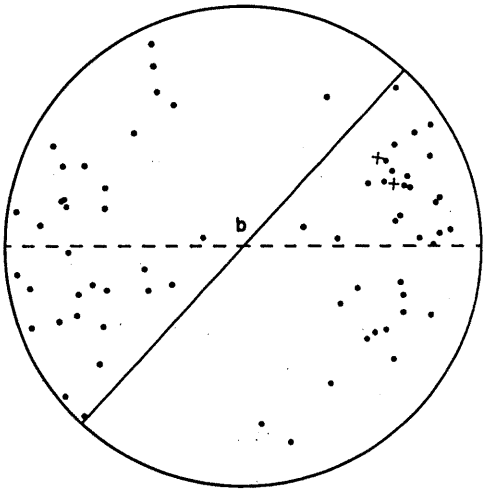

Fig. 25

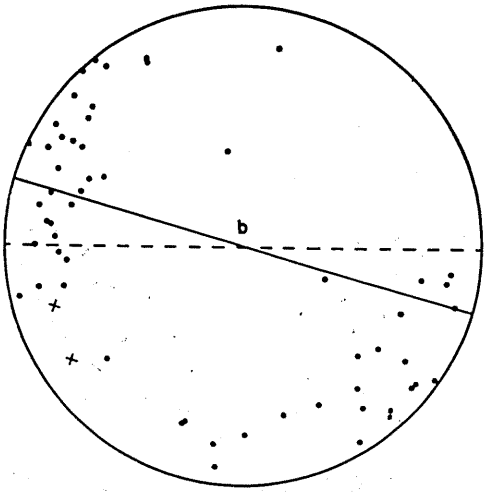

Fig. 26

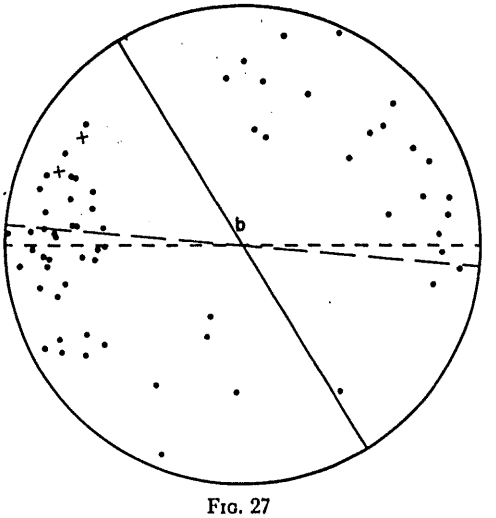

Fig. 27

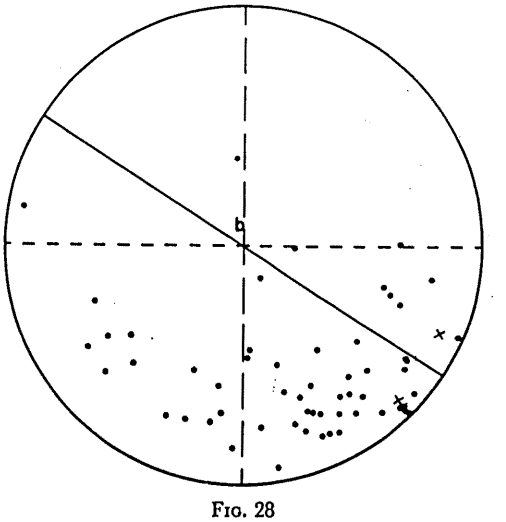

Fig. 28

dency for the girdle to break in such a fashion as the case of Fig. 17. Generally, the c-axis is less concentrated on the girdle II than on the girdle I.

When the c-axis of the host grain (Q_{rc}) lies at high angles to the L_{1-2}-lineation, the c-axis fabric pattern of the subgrains (Q_{rs}) of the first type is characterized by a cleft-girdle, showing a concentration of c-axes on a small circle at ca. 60° to 70° to the L_{1-2}-lineation. For convenience' sake, it is named the girdle II'. The girdle II' (Figs. 24 to 30) is generally incomplete. In Fig. 24, for example, the concentration of c-axes on the girdle II' is quite asymmetric across the projection point of c-axis of the host grain, showing that most c-axes are distributed from the point C, through

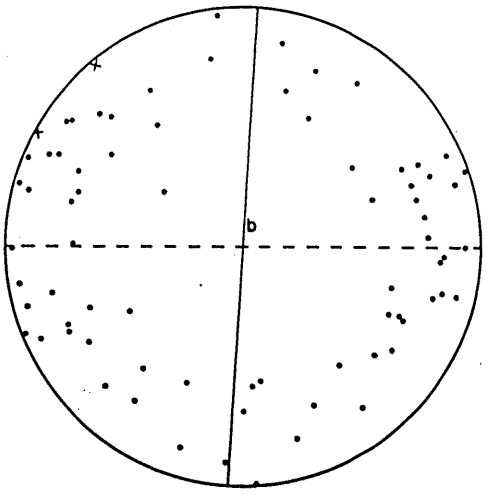

FIG. 29

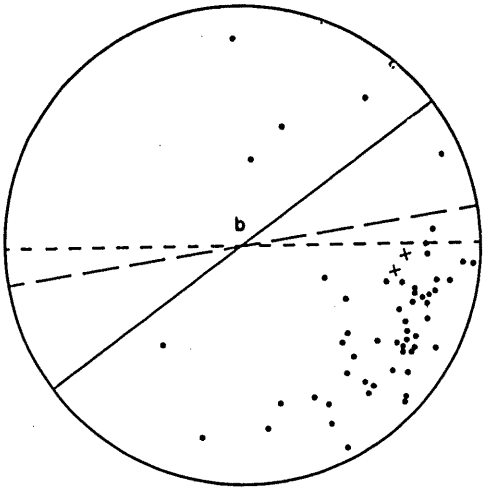

FIG. 30

FIGS. 31 and 32 The c-axis subfabric of Q_{rs}-grains which show the mode of occurrence of the second type. cross: the c-axis of host Q_{rc}-grain.

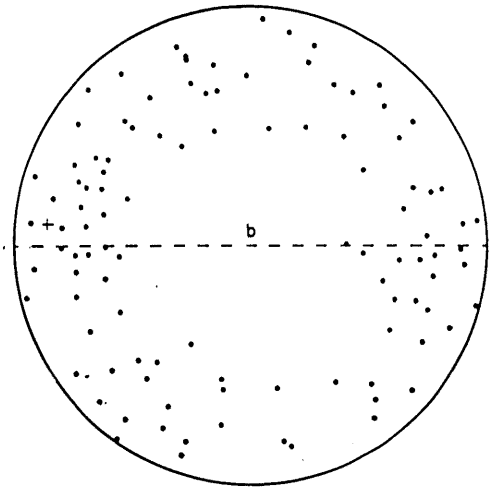

FIG. 31

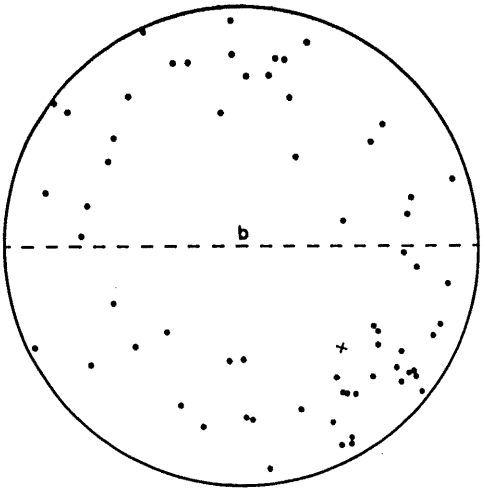

FIG. 32

A, to B on the girdle and between C and B the girdle is completely broken. Also the other diagrams show similar pattern of incomplete girdle, as the case of Fig. 24. The presence of a break on the girdle II' can be compared with the feature of the girdle I for the subgrains whose host crystal is oriented with the c-axis at low to moderate angles to the L_{1-2}-lineation.

Figs. 31 and 32 illustrate the c-axis subfabric for the subgrains which show the mode of occurrence of the second type. The fabric pattern is characterized by a cleft-girdle on a small-circle at ca. 65° to the L_{1-2}-lineation. The small circle girdle of Figs. 31 and 32 does not show the break characteristically developed in the c-axis subfabric diagrams for the subgrains which show the mode of occurrence of the first type.

d) c-axis subfabric for subgrains in vein-quartz (Q_{vs}): The c-axis subfabric for Q_{vs}-grains is illustrated in Figs. 33 and 34. The diagrams have been obtained by measuring Q_{vs}-grains in a quartz vein observed on the ac-section cut from the specimen I. In Fig. 33 there is a distinct girdle with maxima and submaxima on a small circle at ca. 70° to the girdle axis, though the girdle is broken near the direction of the trace of the S_1-surface. The girdle axis coincides with the L_{1-2}-lineation. On the other hand, Fig. 34 shows complete great circle girdle with the girdle axis nearly normal to the S_1-surface. Maximum and submaximum on the girdle are located near the projection points of c-axes of host grains. In Fig. 34, the girdle axis does not coincide with the L_{1-2}-lineation, unlike the case of Fig. 33. Therefore, it can be said that the preferred lattice orientation of Q_{rs}-grains and Q_{vs}-grains is inconsistent with the mesoscopic rock structure from the viewpoint of symmetry.

FIGS. 33 and 34 The c-axis subfabric of Q_{vs}-grains (specimen I). crosses: the c-axis of host grains.

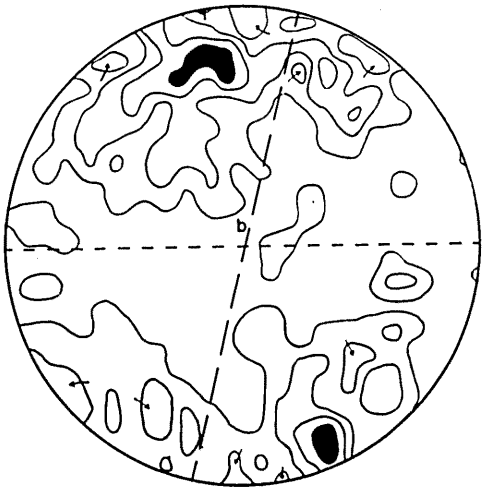

FIG. 33

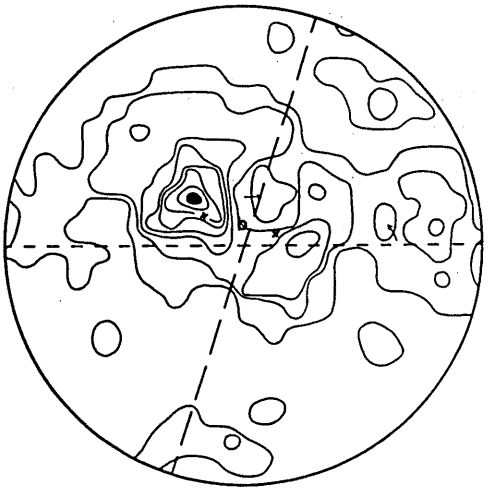

FIG. 34

2) *Dimensional orientation of quartz*

a) Dimensional orientation of quartz phenocryst (Q_{rc}): Quartz phenocrysts in rhyolite pebbles of the specimens I, II and IV do not show any statistically significant grain orientation on the ac-section, bc-section and ab-section (Tables 1, 2 and 4), unlike the case of calcite grains. For the specimen III, the grain orientation on the ac-section is not significant statistically, while on the bc-section and ab-section it is significant statistically (Table 3). On the bc-section the direction of preferred orientation is approximately parallel to the trace of the S_1-surface. On the ab-section it lies at an angle of ca. 32° to the L_{1-2}-lineation. Therefore, quartz phenocrysts in the specimen III show a tendency to orient with the longest axis at an angle of ca. 32° to the L_{1-2}-lineation and parallel to the S_1-surface, but this direction of grain orientation does not coincide with that for calcite grains which is approximately parallel to the L_{1-2}-lineation.

b) Dimensional orientation of quartz grains in quartz-rich pools of the groundmass (Q_{rg}): Results of analysis of dimensional orientation for Q_{rg}-grains on the ac-section, bc-section and ab-section cut from each of the specimens I, II, III and IV are shown in Tables 1, 2, 3 and 4, respectively. For all the specimens, the directions of preferred grain orientation on the ac-section and bc-section are commonly subparallel to the trace of the S_1-surface, while those on the ab-section are commonly subparallel to the L_{1-2}-lineation. Therefore, many Q_{rg}-grains show a tendency to orient with the longest axis in the direction parallel to the L_{1-2}-lineation, the intermediate axis in the direction parallel to the S_1-surface and perpendicular to the L_{1-2}-lineation, and the shortest axis in the direction perpendicular to the S_1-surface, like the case for calcite grains.

c) Dimensional orientation of subgrains in quartz phenocryst (Q_{rs}): Dimensional orientation of Q_{rs}-grains, which show the mode of occurrence of the first type (band) in the individual Q_{rc}-grains, has been analysed only on the ac-section cut from each of the specimens I, II and IV. The results are shown in Table 5. The patterns of grain orientation of Q_{rs}-grains can be divided into three types. In the first type, the grain orientation is not statistically significant. In the second type, the direction of preferred dimensional orientation is approximately parallel to the trace of the S_1-surface, and in the third type, it is approximately perpendicular to the trace of the S_1-surface and parallel to the S_2-surface.

Dimensional orientation of Q_{rs}-grains, which show the mode of occurrence of the second type in the individual Q_{rc}-grains, has been analysed only on the ac-section cut from each of the specimens I, II, III and IV. The patterns of grain orientation are essentially the same as those of Q_{rs}-grains which show the mode of occurrence of the first type, and the former can also be divided into three types, each of which corresponds to respective type of the latter mentioned above.

d) Dimensional orientation of subgrains in vein-quartz (Q_{vs}): Dimensional orientation of Q_{vs}-grains in a quartz vein developed in the specimen 1 has been analysed on the ac-section, bc-section and ab-section. The result is shown in Table 1.

The direction of preferred dimentional orientation on the ac-section is approximately parallel to the trace of the S_2-surface. On the bc-section, it is approximately perpendicular to the trace of the S_1-surface, and, on the ab-section, it is subparallel to the L_{1-2}-lineation. Therefore, many Q_{vs}-grains show a tendency to orient with the longest axis in the direction parallel to the S_2-surface and perpendicular to the L_{1-2}-lineation, the intermediate axis in the direction parallel to the L_{1-2}-lineation and the shortest axis in the direction perpendicular to the S_2-surface, unlike the case of Q_{rg}-grains of the ground-mass.

3) *Distribution of apparent size of quartz*

a) Apparent size of quartz phenocryst (Q_{rc}): Fig. 35 shows the distribution of the apparent size of 200 Q_{rc}-grains, 50 from each of four ac-sections cut from the specimens I, II, III and IV. The apparent size of Q_{rc}-grains is between 0.2 mm and 3.2 mm, with a maximum between 0.3 mm and 0.4 mm.

b) Apparent size of quartz grains in quartz-rich pools of the ground-mass (Q_{rg}): Fig. 36 shows the distribution of apparent size of 200 Q_{rg}-grains, which are a part of the Q_{rg}-grains used for c-axis subfabric diagrams shown in Figs. 11, 13, 14 and 15, 50 from each of four specimens. Q_{rg}-grains having the apparent sizes as shown in Fig. 36 occupy more than 90 per cent of total number of Q_{rg}-grains in the quartz-rich pools of the ground-mass, where the c-axis subfabric diagrams shown in Figs. 11, 13, 14, 15 and 16 were obtained. The apparent size in question is between 0.006 mm and 0.03 mm, with a marked maximum between 0.01 mm and 0.015 mm. The Q_{rg}-grains of apparent size of 0.03 mm correspond approximately to those of the maximum apparent size observed in the quartz-rich pools in question. The apparent size of Q_{rg}-grains is commonly smaller than one tenth of that of Q_{rc}-grains.

c) Apparent size of subgrains in quartz phenocrysts (Q_{rs}): Fig. 37 shows the distribution of apparent size of 300 Q_{rs}-grains in the specimens I, II and IV, which are present in bands (the mode of occurrence of the first type) in which the Q_{rs}-grains are preferably oriented subparallel to the trace of the S_1-surface on the ac-section. The apparent size of Q_{rs}-grains in question is smaller than 0.09 mm, with a maximum between 0.02 mm and 0.03 mm. Therefore, the most frequent apparent size of Q_{rs}-grains is twice as large as that of Q_{rg}-grains shown in Fig. 36.

Fig. 38 shows the distribution of apparent size of 300 Q_{rs}-grains in the specimens I, II, III and IV, which are present in marginal to internal parts of Q_{rc}-grains (the mode of occurrence of the second type), where Q_{rs}-grains are preferably oriented subparallel to the trace of the S_1-surface on the ac-section. The apparent size of Q_{rs}-grains in question is smaller than 0.1 mm, with a maximum between 0.02 mm and 0.03 mm. The character of apparent grain size distribution shown in Fig. 38 is closely similar to that shown in Fig. 37.

The textural features (c-axis subfabric, dimensional subfabric and apparent grain size) of Q_{ss}-grains in the psammitic matrix are essentially the same as those of Q_{rs}-grains in the rhyolite pebble examined above.

d) Apparent size of subgrains in vein-quartz (Q_{vs}): Fig. 39 shown the distribu-

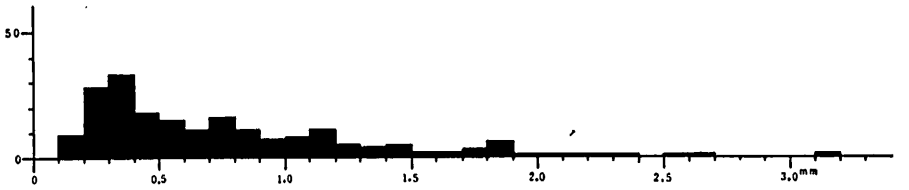

FIG. 35 Distribution of the apparent size of 200 Q_{rc}-grains in the rhyolite pebble as measured on the ac-sections. The frequency is given by number of grains.

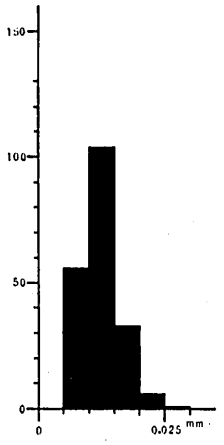

FIG. 36 Distribution of the apparent size of 200 Q_{rg}-grains which are fraction of Q_{rg}-grains for the c-axis subfabric diagrams shown in Figs. 11, 13, 14 and 15. The frequency is given by number of grains.

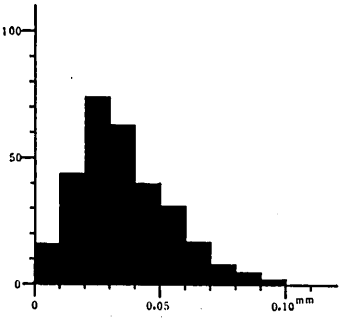

FIG. 37 Distribution of the apparent size of 300 Q_{rs}-grains (in the specimens I, II and IV), which are present in bands in which those grains are preferably oriented subparallel to the trace of the S_1-surface on the ac-sections. The frequency is given by number of grains.

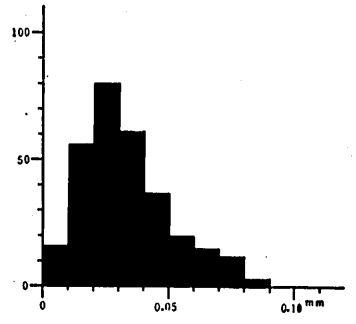

FIG. 38 Distribution of the apparent size of 300 Q_{rs}-grains (in the specimens I, II and IV), which are present in marginal to internal parts of Q_{rc}-grains (the mode of occurrence of the second type) in which those grains are preferably oriented subparallel to the trace of the S_1-surface on the ac-sections. The frequency is given by number of grains.

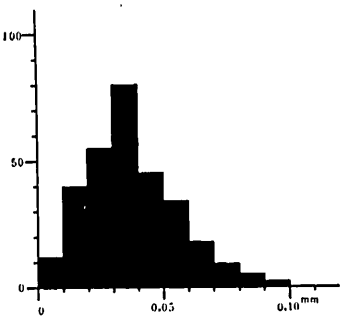

FIG. 39 Distribution of the apparent size of 300 Q_{vs}-grains (in the specimen I) as measured on the ac-section. The frequency is given by number of grains.

tion of apparent size of 300 Q_{vs}-grains in a quartz vein in the specimen I, measured on the ac-section. The apparent size is smaller than 0.10 mm, with a maximum between 0.03 mm and 0.04 mm. The value (0.03 mm to 0.04 mm) is larger than that of the apparent size of Q_{rs}-grains showing the maximum frequency.

D. Quartz Subfabrics of Psammitic Matrix

1) *c-axis subfabric of quartz*

a) c-axis subfabric of coarse-grained clastic quartz (Q_{sc}): .The c-axis subfabric diagrams shown in Figs. 40 and 41 are based on the measurement of 200 grains on the ac-section for each of the specimens V and VI. No preferred orientation is detectable in the diagrams.

b) c-axis subfabric of fine-grained quartz (Q_{rg}): The c-axis subfabric for 200 grains observed on the ac-section cut from each of the specimens V and VI is illustrated in Figs. 42 and 43, respectively. In both diagrams there is a distinct cleft-girdle with maxima and submaxima on a small circle at ca. 60° to the girdle axis, which coincides with the L_{1-2}-lineation and with the direction of grain elongation which will be statistically examined in the later pages. The pattern of fabric diagrams shown in Figs. 42 and 43 is essentially the same as that for Q_{rg}-grains and calcite grains in the rhyolite pebbles (specimens I, II and III).

c) c-axis subfabric of quartz of pressure-shadows (Q_{sf}): Figs. 44 to 47 show the c-axis orientation of measurable Q_{sf}-grains found in four pressure-shadows on the ab-sections of specimens V and VI, respectively. The number of the measurable Q_{sf}-grains is less than 70 per cent of the total number of Q_{sf}-grains observed in any single shadow. In each diagram the solid line indicates the trace of quartz face

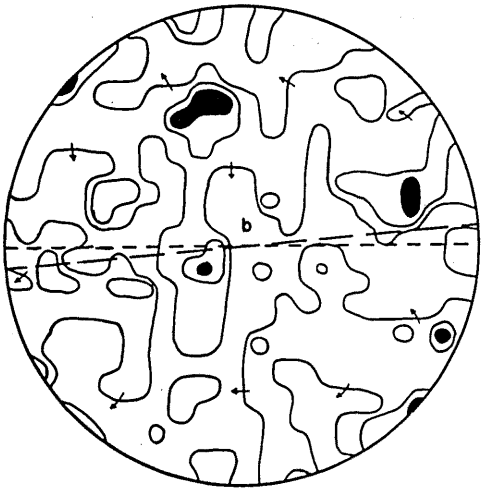

Fig. 40 The c-axis subfabric of 200 Q_{sc}-grains in the psammitic matrix (specimen V). Contours: 3-2-1 %.

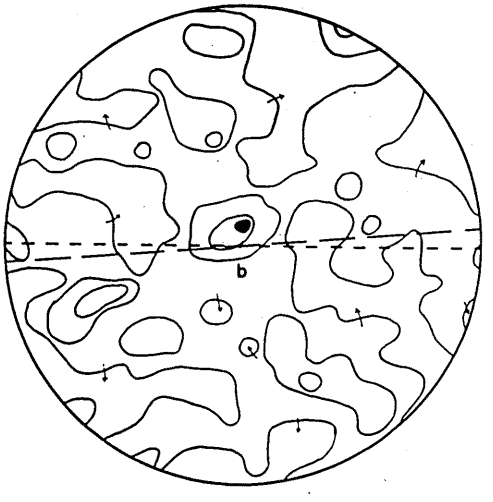

Fig. 41 The c-axis subfabric of 200 Q_{sc}-grains in the psammitic matrix (specimen VI). Contours: 4-3-2-1 %.

for pressure-shadow on the ab-section. Although the c-axes of Q_{sf}-grains tend to be preferably oriented in each diagram, any regular relationship can not be found between the diagrams (Figs. 44, 45, 46 and 47) with respect to the position of c-axis concentration. Therefore, it may be said that for the lattice orientation of quartz grains in the pressure-shadows there is no constant relation. This conclusion coincides with that of Pabst (1931), but not with the conclusion of Fisher (1926) that the

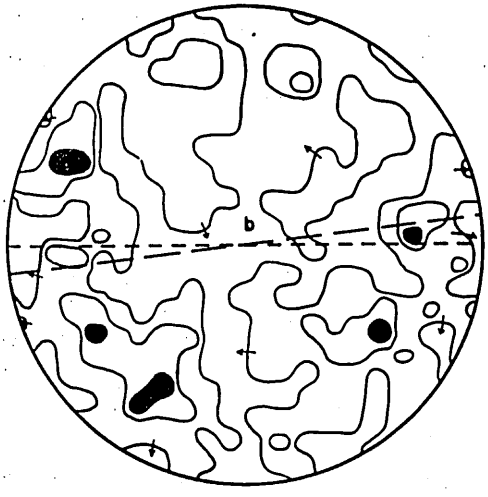

FIG. 42 The c-axis subfabric of 200 Q_{sg}-grains in the psammitic matrix (specimen V). Contours: 3-2-1 %.

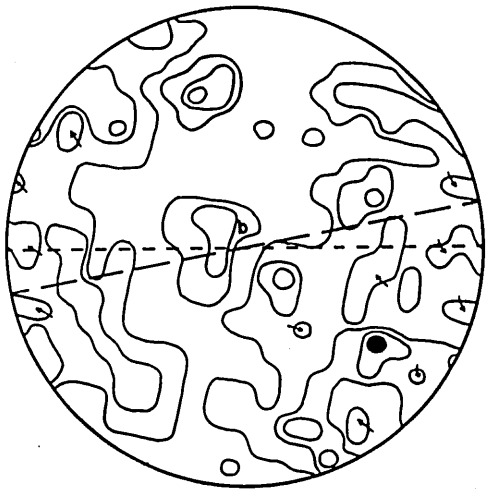

FIG. 43 The c-axis subfabric of 200 Q_{sg}-grains in the psammitic matrix (specimen VI). Contours: 4-3-2-1 %.

FIGS. 44 to 47 The c-axis orientation of measurable Q_{sf}-grains found in the pressure-shadow on the ab-section (from the specimens V and VI). solid line: the trend of controlling quartz face. cross: the c-axis of controlling Q_{sc}-grain.

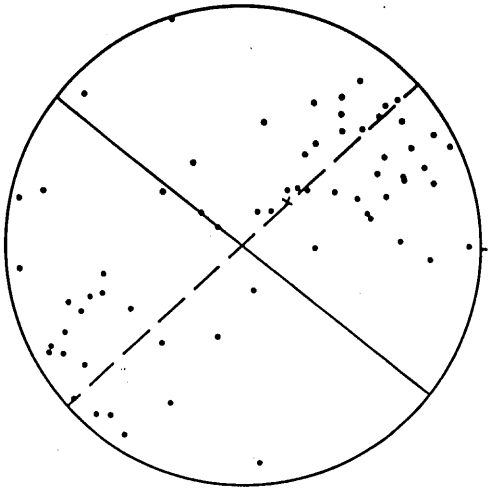

FIG. 44

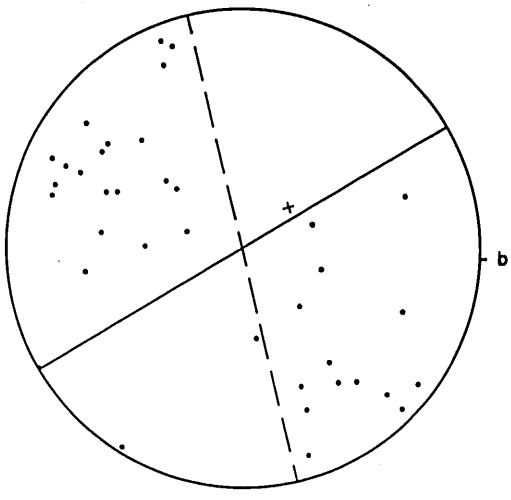

FIG. 45

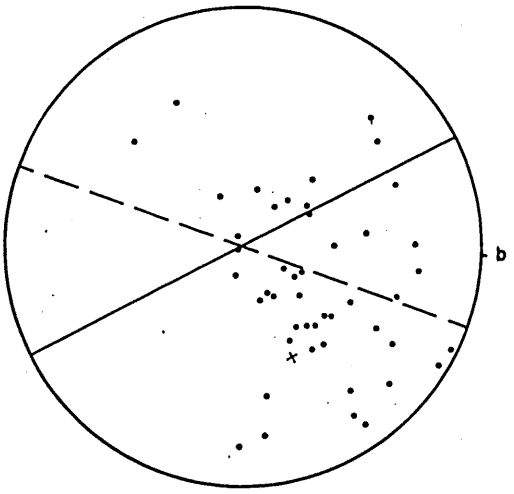

FIG. 46

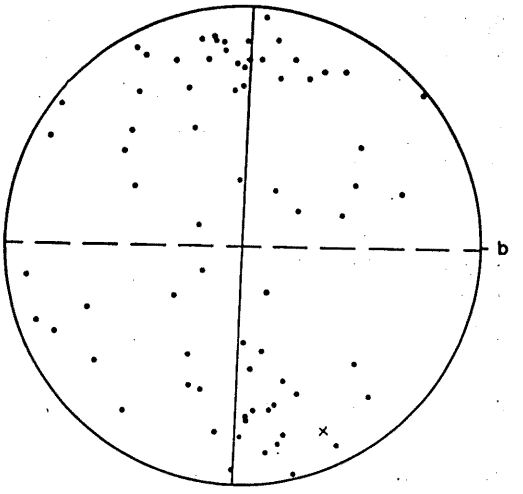

FIG. 47

c-axis of quartz in the pressure-shadow shows a tendency to be oriented perpendicular to the controlling crystal face. As is obvious in Figs. 44 to 47, there is no constant relation between the elongation direction and the c-axis for Q_{sf}-grains.

2) *Dimensional orientation of quartz*

a) Dimensional orientation of coarse-grained clastic quartz (Q_{sc}): For Q_{sc}-grains of the specimens V and VI, the directions of preferred dimensional orientation on the ac-section and bc-section are subparallel to the trace of the S_1-surface (Tables 1 and 4), while on the ab-section they are not significant statistically. Therefore, it can be concluded that many Q_{sc}-grains in the psammitic matrix tend to orient with the shortest axis perpendicular to the S_1-surface and with the longest axis in random directions within the S_1-surface.

b) Dimensional orientation of fine-grained quartz (Q_{sg}): The results of analysis of dimensional orientation of Q_{sg}-grains observed on the ac-section, bc-section and ab-section cut from the specimens V and VI are shown in Tables 1 and 4, respectively. The directions of preferred dimensional orientation on the ab-section and bc-section are subparallel to the trace of the S_1-surface, while those on the ab-section are subparallel to the L_{1-2}-lineation. Therefore, it can be concluded that many Q_{rs}-grains tend to orient with the longest axis in the direction parallel to the L_{1-2}-lineation, the intermediate axis in the direction parallel to the S_1-surface and perpendicular to the L_{1-2}-lineation and the shortest axis in the direction perpendicular to the S_1-surface, unlike the case of Q_{sc}-grains. The pattern of dimensional orientation of Q_{sg}-grains is identical with that of calcite and Q_{rg}-grains in the rhyolite pebbles.

c) Dimensional orientation of quartz of pressure-shadows (Q_{sf}): As observed on the ac-section and bc-section, growth of pressure-shadows surrounding Q_{sc}-grains appears to be maximum in the direction parallel to the S_1-surface and minimum (generally absent) in the direction perpendicular to the S_1-surface. However, devel-

opment of pressure-shadows is more clearly observed on the ab-section than on the ac-section and bc-section. When observed on the ab-section, pressure-shadows grow radially in all direction around Q_{sc}-grains (Plate 2-2), but their growth tends to be maximum in the direction parallel to the L_{1-2}-lineation and minimum in the direction perpendicular to the L_{1-2}-lineation.

The results of analysis of dimensional orientation of quartz grains in four pressure-shadows, whose c-axis subfabric was examined in the preceding page (Figs. 44 to 47), are shown in Table 6. The orientations of the longest axis of Q_{sf}-grains on the ab-section are commonly significant statistically with high probability. The orientation directions are inclined at moderate to high angles to the controlling quartz face. The dimensional orientations of Q_{sf}-grains in other pressure-shadows observed on the ab-sections cut from the specimen V and VI are so striking that they hardly require any statistical measurement, and the assumed orientation directions of Q_{sf}-grains are generally inclined at moderate to high angles to the controlling quartz face.

3) *Distribution of apparent size of quartz*

a) Apparent size of coarse-grained clastic quartz (Q_{sc}): Fig. 48 shows the distribution of apparent size of 100 Q_{sc}-grains, 50 from each of two ac-sections cut from the specimens V and VI. The apparent size of Q_{sc}-grains is between 0.16 mm and 1.00 mm, with a maximum between 0.3 mm and 0.4 mm.

b) Apparent size of fine-grained quartz (Q_{sg}): Fig. 49 shows the distribution of apparent size of 200 Q_{sg}-grains measured on the ac-section cut from the specimen V, whose c-axis subfabric was examined in the preceding page (Fig. 42). The apparent size is smaller than 0.02 mm, showing a maximum frequency between 0.005 mm and 0.01 mm. The number of the Q_{sg}-grains having the apparent size corresponding to Fig. 49 occupy more than 90 per cent of the total number of Q_{sg}-grains observed in the part of ground-mass, where the c-axis subfabric and the apparent

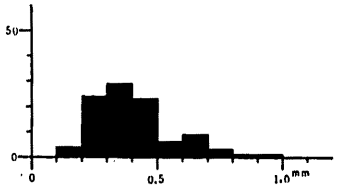

FIG. 48 Distribution of the apparent size of 100 Q_{sc}-grains in the psammitic matrix as measured on the ac-sections. The frequency is given by number grains.

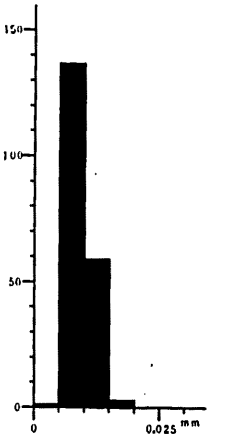

FIG. 49 Distribution of the apparent size of 200 Q_{sg}-grains observed on the ac-section cut from the specimen V, whose c-axis subfabric is shown in Fig. 42. The frequency is given by number of grains.

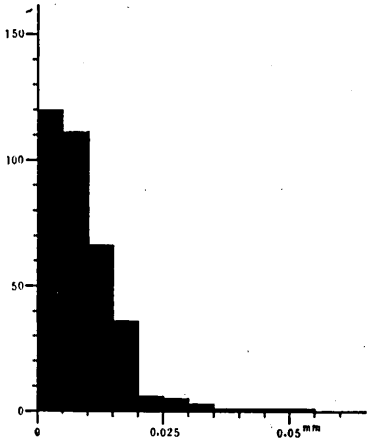

FIG. 50 Distribution of the apparent size of 350 Q_{sf}-grains measured on the ab-section for the specimen V. The frequency is given by number of grains.

size distribution for Q_{sg}-grains shown in Fig. 42 and 49 were examined. The value of the most frequent apparent size of Q_{sg}-grains is smaller than that of Q_{rg}-grains in the ground-mass of rhyolite pebbles.

c) Apparent size of quartz of pressure-shadows (Q_{sf}): Fig. 50 shows the distribution of apparent size of 350 Q_{sf}-grains measured on the ab-section for the specimen V. The apparent size is smaller than 0.055 mm, showing a maximum frequency of Q_{sf}-grains having the apparent size smaller than 0.005 mm, whose value is smaller than that for Q_{sg}-grains.

The textural features (c-axis subfabric, dimensional subfabric and apparent grain size) of feather quartz of pressure-shadows surrounding Q_{rc}-grains in the rhyolite pebbles are essentially the same as those surrounding Q_{sc}-grains in the psammitic matrix described above.

IV. CONSIDERATIONS

Quartz phenocrysts (Q_{rc}) in rhyolite pebbles and coarse-grained clastic quartz (Q_{sc}) in psammitic matrix of the conglomerate do not show any preferred lattice orientation (Figs. 7 to 10 and Figs. 40 and 41), while quartz grains (Q_{rg}) in quartz-rich pools of the ground-mass of rhyolite pebbles and fine-grained quartz grains (Q_{sg}) in psammitic matrix show marked preferred orientation (Figs. 11 to 16 and Figs. 42 and 43). The single symmetry axis of the c-axis subfabric diagrams of the latter coincides, in general, with that of mesoscopic rock structure, i.e. the L_{1-2}-lineation, as well as with the fold axis of the major anticlinal structure. It would safely be assumed that the c-axis subfabric for these fine-grained quartz (Q_{rg}-grains and Q_{sg}-grains) originated during the deformation responsible for the formation of mesoscopic rock structure and major structure, that is, the S_1-deformation and the S_2-deformation.

What causes are related to the discrepancies between the fabric pattern for Q_{rc}-

grains and that for Q_{rg}-grains in the rhyolite pebbles and between that for Q_{sc}-grains and that for Q_{sg}-grains in the psammitic matrix? The mechanism by which preferred lattice orientation for Q_{rg}-grains and that for Q_{sg}-grains were developed did not affected the random lattice orientation of Q_{rc}-grains and Q_{sc}-grains inherited from their original rocks. There are some types of mechanisms by which preferred orientation of mineral lattice characteristically developed in metamorphic tectonites can develop directly or indirectly as result of stress, as many authors (e.g. FLINN, 1965) has pointed out. Which of those mechanisms is related to the development of preferred lattice orientation of Q_{rg}-grains and Q_{sg}-grains?

In syntectonically recrystallized quartz aggregates produced experimentally has been produced a high degree of preferred orientation of quartz lattice (GRIGGS, *et al.*, 1960; DELITSIN, 1962; CARTER, *et al.*, 1964; RALEIGH, 1965). The problem on the preferred orientation of mineral lattice due to recrystallization under non-hydrostatic stress field has been considered from the thermodynamic viewpoint by many authors (KAMB, 1959 and 1961; MACDONALD, 1957, 1960 and 1961; BRACE, 1960; KUMAZAWA, 1963). It seems to be generally agreed that elastic property of quartz is sufficiently anisotropic to induce a thermodynamically stable preferred lattice orientation for quartz aggregate recrystallized under non-hydrostatic stress field. There are two types of mechanisms, which may give rise to a thermodynamically stable orientation during recrystallization of crystalline material, that is, nucleation which creates new grains in a thermodynamically favoured attitude, and grain-boundary migration which eliminates grains in an unfavoured attitude, as previously considered by many authors. If it is assumed that the preferred lattice orientation of Q_{rg}-grains and Q_{sg}-grains was developed by those diffusion mechanisms, then the significance of discrepancy between the pattern of c-axis subfabric for Q_{rg}-grains and Q_{sg}-grains and that for Q_{rc}-grains and Q_{sc}-grains seems to be more reasonablly illustrated than it is done by the application of other orienting mechanism.

The apparent size of Q_{rg}-grains and that of Q_{sg}-grains (Figs. 36 and 49), which were derived from the very fine-grained materials of ground-mass of the rhyolite pebbles and psammitic matrix respectively, are generally smaller than one tenth of that of Q_{rc}-grains and Q_{sc}-grains which correspond originally to quartz phenocrysts in the rhyolite pebbles and coarse-grained clastic quartz in the psammitic matrix, respectively. It is clear that, at the beginning of S_1-deformation, the original quartz grains of the ground-mass were smaller in size than Q_{rg}-grains and Q_{sg}-grains. According to the results of syntectonic recrystallization of flint and quartzite experimentally given by CARTER *et al.* (1964), under the conditions in which the original flint consisting of very fine-grained quartz was completely replaced by a quartzite consisting of coarser-graind quartz induced by recrystallization, the original quartzite consisting of relatively coarse-grained quartz was not entirly replaced by new grains but the formation of new grains were generally restricted to domains near the boundaries of deformation bands and grains (only to highly strained domain). And "the amount of grain-boundary energy in the cryptocrystalline flint seems to be sufficiently

large to promote recrystallization under hydrostatic stress at 1,000° C. In the relatively coarse-grained quartzite, however, additional free energy derived from strain induced in the grains seems to be required for recrystallization to take place under these conditions" (CARTER, *et al.*, 1964, pp. 727–728). It would be assumed that, during the S_1-deformation and S_2-deformation, the total amount of grain-boundary energy and strain energy for the very fine-grained quartz grains of the ground-mass of the rhyolite pebbles and psammitic matrix was sufficiently large for those grains to be completely replaced by new grains (Q_{rg}-grains and Q_{sg}-grains) by recrystallization, while these energies for the coarse-grained quartz phenocrysts and clastic quartz grains were not sufficiently large for those grains to be completely replaced by new grains.

Q_{rg}-grains in the rhyolite pebbles and Q_{sg}-grains in the psammitic matrix show commonly a preferred dimensional orientation symmetrically consistent with the mesoscopic rock structure in such a fashion as many of them tend to orient with the longest axis in the direction parallel to the L_{1-2}-lineation, the intermediate axis in the direction parallel to the S_1-surface and perpendicular to the L_{1-2}-lineation and the shortest axis in the direction perpendicular to the S_1-surface. This pattern of dimensional orientation of Q_{rg}-grains and Q_{sg}-grains is essentially the same as that of calcite grains in the rhyolite pebbles, but it is quite different from that of Q_{rc}-grains and Q_{sc}-grains. Q_{rc}-grains in three rhyolite pebbes show no preferred dimensional orientation, and those in one rhyolite pebble show an orientation with the direction of vector mean oblique (32°) to the L_{1-2}-lineation, being asymmetric to the mesoscopic rock structure. In the psammitic matrix, many Q_{sc}-grains show a tendency to orient with the shortest axis in the direction perpendicular to the S_1-surface and with the longest axis in random directions within the S_1-surface.

In his investigation on the deformation of the Funzie conglomerate, FLINN (1965) has revealed that individual quartz grains have a form similar to that of their parent pebble and that the major form axes of the grains are oriented similarly to the pebble axes. Analogous relationship between the form of deformed pebble and that of constituent quartz grain was observed also in the quartzite pebbles of Central Vermont by BRACE (1955). The strain in the deformed pebble may be regarded as statistically homogeneous, the mean strain of the system concerned being represented by an ellipsoid. The from of deformed pebble itself may be regarded as strain ellipsoid (e.g., OFTEDAHL, 1948; FLINN, 1956). Deformation by diffusion processes, say the Riecke diffusion, would result in grains of the same shape as the strain ellipsoid corresponding to the mean strain of the system concerned, if they were originally eqidimensional. On this assumption, FLINN (1956, p. 493) says, "the shapes of the grain are best explained on Riecke Principle." On the basis of analogous assumption, the senior author (HARA; 1966 a and b, in press) interpreted the dimensional subfabric of quartz in flexural folds, giving the results consistent with informations concerning mechanisms of flexural folding based on the theoretical and experimental investigations.

FAIRBAIRN (1950) has shown experimentally that the quartz grains in a synthetic quartzite developed forms with their longest axis perpendicular to the compression axis and the shortest axis parallel to it. Analogous observations were made for quartz grains in the syntectonically recrystallized flint and quartzite experimentally given by CARTER *et al.* (1964).

According to the knowledge of experimental studies on metalic and non-metalic minerals (cf., DORN, 1961; KINGERY, 1960), under physical conditions where recrystallization can occur, mechanisms contributing to creep deformation include climbing of dislocations, Nabarro-Herring diffusion and flow of grain boundaries, in addition to translation gliding and twinning. Under analogous physical conditions Riecke diffusion is likely to take place as deformation process of silicate minerals (RAMBERG, 1952; FLINN, 1965). Generally, the mechanisms, by which deformed grains would develop the same form as the strain ellipsoid corresponding to the mean strain of the system concerned, if they were originally equiaxial, include translation gliding, Nabarro-Herring diffusion, Riecke diffusion and grain-boundary migration (FLINN, 1965). Which of those mechanisms is related to the formation of preferred dimensional orientation of Q_{rg}-grains and Q_{sg}-grains?

Q_{vs}-grains show a tendency to orient with the longest axis in the direction parallel to the S_2-cleavage and perpendicular to the L_{1-2}-lineation, the intermediate axis in the direction parallel to the L_{1-2}-lineation and the shortest axis in the direction perpendicular to the S_2-cleavage, unlike the case of Q_{rg}-grains and Q_{sg}-grains. Analogous pattern of dimensional orientation of Q_{vs}-grains appears to be developed also in some other quartz veins in the crystalline schists of the Oboke district (Plate 10-1 and 2). The geometric relationship between the S_2-cleavage and the dimensional orientaiton of Q_{vs}-grains mentioned above is quite similar to that between the cleavage and the dimensional orientation of deformed öoides described by CLOOS (1947). In the latter case, the form of deformed öoide itself may be regarded as a strain ellipsoid.

Q_{vs}-grains are subgrains in coarse-grained quartz of quartz veins. There are two types of mechanisms, by which subgrains can be developed in a single grain, that is, polygonization and nucleation-grain growth. The orientation of subgrain-boundary due to polygonization is generally dependent upon the orientation of glide direction on active glide plane in the grain, following to the knowledge of experimental studies on metals (CAHN, 1950; MCLEAN, 1951 and 1952). It is unlikely that subgrains of quartz produced by polygonization develop the same form as the strain ellipsoid corresponding to the mean strain of the system concerned. During syntectonic recrystallization, recovery including polygonization may be also taking place within the strained grains. It may be therefore said that most Q_{vs}-grains originated by nucleation and subsequent grain growth in the vein-quartz, accompanied with deformation of the grain shape, that is responsible for the formation of dimensional subfabric, during the S_2-deformation, though some Q_{vs}-grains were produced as result of polygonization.

Q_{rs}-grains in each Q_{rc}-grain and Q_{ss}-grains in each Q_{sc}-grain show either one of following three types of dimensional orientation as examined on the ac-section, that is, 1) the preferred dimensional orientation in the direction parallel to the S_1-surface, 2) the preferred orientation in the direction parallel to the S_2-surface, 3) random orientation. The former two suggest that the subgrains (Q_{rs}-grains and Q_{ss}-grains) were formed due to the mechanisms of nucleation and subsequent grain growth during the S_1-deformation and the S_2-deformation respectively, accompanied with deformation of the grain shape. The fact that these subgrains are present only within narrow bands in some Q_{rc}-grains (or Q_{sc}-grains), terminating within the grain-boundaries (the first type of mode of occurrence), would suggest that the deformation of those Q_{rc}-grains (or Q_{sc}-grains) were concentrated within those bands, presumably kink bands, during the S_1-deformation and S_2-deformation, and the strain enegy stored in those parts would have contributed to polygonization and/or nucleation-grain growth.

The character of the girdle I in the c-axis subfabric diagrams for Q_{rs}-grains in Q_{rc}-grain, whose c-axis is inclined at low to moderate angles to the L_{1-2}-lineation, appears to be consistent with the assumption that the bands consisting of Q_{rs}-grains originated from kink bands in the host crystals. The distribution of c-axes on the girdle I is quite asymmetric across the projection point of the c-axis of the host Q_{rc}-grain, showing a tendency to develop a distinct break in such a fashion as clearly shown in Fig. 17. X-ray studies on naturally deformed quartz, which shows undulatory extinction, deformation lamellae, marginal granulation and fracturing, have revealed that the axis of lattice bending coincides with either one of the a-axis and a'-axis (HERITSCH and PAULITSCH, 1954; BAILEY, BELL and PENG, 1958; PAULITSCH and AMBS, 1963). It is considered that attitude of the girdle I reflects the original change in orientation of c-axis from the host crystal to the kink band, and that the sence of rotation from the projection point of c-axis of the host Q_{rc}-grain to the portion of c-axis concentration on the girdle I would indicate the original sense of rotation of c-axis from the host crystal to kink band.

The axis of the gridle II coincides generally with the symmetry axis of mesoscopic rock structure, the L_{1-2}-lineation. In static recrystallization of strained grains, nuclei may develop with a preferred lattice orientation closely related to the host lattice (GRIGGS *et al.*, 1960), while in syntectonic recrystallization, nuclei may develop with their lattice in an attitude symmetrically consistent with the stress system acting on the system concerned, regardless of the orientation of host lattice (GRIGGS *et al.*, 1960; HEARD, 1963; FERREIRA *et al.*, 1964). On the basis of above described characteristics of the girdle I and girdle II, therefore, one might suppose that Q_{rs}-grains showing c-axis distribution on the girdle I were produced within the original kink bands by static recrystallization, while Q_{rs}-grains showing c-axes for the girdle II were induced by syntectonic recrystallization. During static or syntectonic recrystallization, generally, recovery including polygonization may be also taking place within the strained grains, forming a network of subgrain-boundaries which separate

clearly subgrains with different lattice orientation. It has been stated that lattice orientation of subgrains produced as result of polygonization is generally dependent upon the orientation of active glide plane in the host grain, on studies of metals. Alternatively, therefore, one might assume that Q_{rs}-grains having c-axes for the girdle I were produced as result of polygonization by syntectonic recovery, while Q_{rs}-grains having c-axes for the girdle II were produced by syntectonic nucleation and subsequent grain growth. In the c-axis subfabric diagrams of Figs. 18 and 19, only a single girdle, the girdle I, is discernible. However, Q_{rs}-grains for Fig. 18 show a preferred dimensional orientation with their long axes subparallel to the trace of the S_1-surface, and those for Fig. 19 show a preferred dimensional orientation with their long axes subparallel to the trace of the S_2-surface, as measured on the ac-section. It has been assumed that Q_{rs}-grains showing the dimensional subfabric of the former type originated during the S_1-deformation and Q_{rs}-grains showing the dimensional subfabric of the latter type originated during the S_2-deformation commonly due to nucleation and subsequent grain growth. Therefore, it seems most probable to conclude that Q_{rs}-grains having c-axes for the girdle I as well as those for the girdle II were commonly produced within the kink bands in Q_{rc}-grains by syntectonic recrystallization. The formation of kink bands in Q_{rc}-grains suggests that the process of deformation of them involve generally translation gliding on a special crystallographic plane which is inclined at high angles to the bands (cf. BARRETT, 1952; TURNER, *et al.*, 1954; CHRISTIE, *et al.*, 1964). This conclusion would be valid to the formation of Q_{rs}-grains in Q_{rc}-grains, whose c-axes are inclined at high angles to the L_{1-2}-lineation, and also to the formation of Q_{rs}-grains which show the mode of occurrence of the second type. Therefore, it may be said that the deformation of Q_{rc}-grains occurred by the translation gliding on a particular crystallographic plane, accompanied with syntectonic recrystallization in highly strained parts (the formation of new grains = Q_{rs}-grains). Like phenomenon occurred also in the deformation of Q_{sc}-grains during the S_1-deformation and S_2-deformation.

There are pressure-shadows of feather quartz and white mica surrounding coarse-grained Q_{rc}-grains and Q_{sc}-grains. The pressure-shadows are generally elongated in a plane parallel to the S_1-schistosity. As observed on the ab-section, pressure-shadows appear to develop in all directions around Q_{rc}-grains (or Q_{sc}-grains). Broadly speaking, the distribution of the maximum diameter of the pressure-shadow (presumably = direction of maximum growth = direction of maximum extension) around individual Q_{rc}-grains and Q_{sc}-grains tend to be parallel to the L_{1-2}-lineation. It has been stated that the development of pressure-shadows is controlled by the extension acting parallel to the plane of their growth, which pulls the matrix from the sides of the porphyritic crystals (PABST, 1931; MÜGGE, 1928; TURNER *et al.*, 1963). According to this belief, the strain picture for pressure-shadows in question is quite consistent with that for the dimensional subfabric of Q_{rg}-grains and Q_{sg}-grains. It can be assumed that the deformation related to the formation of the pressure-shadows was resposible for the formation of the S_1-schistosity.

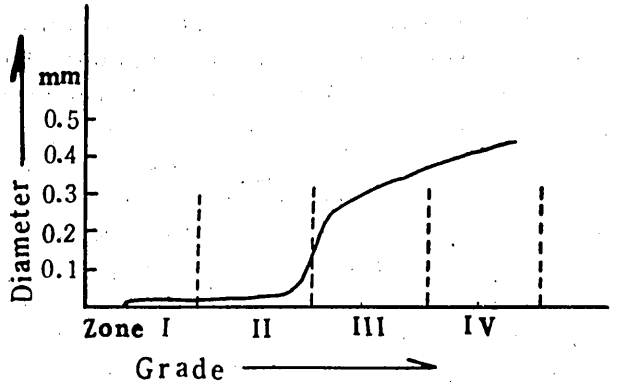

FIG. 51 Schematic diagram showing the average grain sizes of quartz in siliceous schists of various metamorphic grades in the Kôtsu-Bizan district (after IWASAKI, 1963).

The grain size of quartz in the Sambagawa crystalline schists (siliceous schist) of various metamorphic grades was examined by IWASAKI (1963) in the Kôtsu-Bizan district, giving the result reproduced in Fig. 51. "It is seen from the figure that the grain size of quartz in quartz schists generally increase with increasing grade of metamorphism, and that the difference of the grain size is conspicuous between zones II and III. In zone III, the grain size of quartz becomes about ten times as large as that of zone II" (IWASAKI, 1963, p. 36). In the crystalline schsits of the zones III and IV are commonly found porphyroblasts of sodic plagioclase. The boundary between zones II and III in which the average grain size of quartz begins to increase abruptly is also that in which porphyroblasts of sodic plagioclase begin to be abruptly found. In the crystalline schists of the zones III and IV are not found porphyroblasts of quartz. Quartz grains in the siliceous schists of the zone III and IV show preferred lattice orientation (NAKAYAMA, 1964), whose pattern is essentially the same as that of the c-axis subfabric for Q_{rg}-grains and Q_{sg}-grains of the Oboke conglomerate schist. The average size of quartz grains in the zone IV is nearly equal to that of Q_{sc}-grains, whose c-axis subfabric shows no preferred orientation. The metamorphic grade of the conglomerate schist of the Oboke district corresponds to that of the zone II of the Kôtsu-Bizan district. The average size of Q_{rg}-grains and Q_{sg}-grains is approximately equal to that of quartz grains of siliceous schists showing the metamorphic grade of the lower part of zone II in the Kôtsu-Bizan district. The textural features of the recrystallized ground-mass consisting of Q_{rg}-grains (or Q_{sg}-grains) (plate 7-2) appear to be correlated with those produced as result of primary recrystallization and subseqent grain growth in experimental annealing of metals.

On the basis of above descriptions and considerations, it is assumed that, when metamorphic deformation induced preferred lattice and dimensional orientations to the fine-grained quartz (Q_{rg}-grains and Q_{sg}-grains), deformation of the porphyritic quartz (Q_{rc}-grains and Q_{sc}-grains) occurred by translation gliding on a certain crystallographic plane, accompanied with the formation of kink bands and recrystalliza-

tion of those bands and grain-boundaries, though no preferred lattice and dimensional orientations were induced to those coarse-grained quartz grains. Obtained data inclines our mind to such a view that for the deformation of quartz taking place under metamorphic conditions diffusion mechanisms, including nucleation, grain-boundary migration and Riecke diffusion, play the more predominant role than translation gliding on some particular crystallographic planes does, though CHRISTIE *et al.* (1964) and CHRISTIE and GREEN (1964) found several slip mechanisms in quartz and GRIGGS and BLACIC (1964 and 1965) found that the strength of quartz drops to very low stress levels in the presence of small amount of H_2O. The problem on the deformation mechanisms of quartz taking place under metamorphic conditions seems to have mainly so far been considered in such a way to clarify orientation patterns of quartz lattice in metamorphic tectonites and orienting mechanisms responsible for the orientation patterns, with regard to homogeneity, symmetry and detail of pattern such as maxima, minima and girdles in the individual diagrams. The view that under metamorphic conditions deformation of quartz occurs mainly by translation gliding and fracturing on some particular crystallographic planes was popular for a long time (e.g., SANDER, 1930 and 1950; SCHMIDT, 1932; KNOPF and INGERSON, 1938; FAIRBAIRN, 1949; KOJIMA and HIDE, 1958). Recently, FLINN (1965) discussed in detail possible deformation mechanisms of rocks and minerals taking place under metamorphic conditions. The popular view that under metamorphic conditions deformation of rocks takes generally place by translation gliding and twinning in constituent minerals was questioned. He (p. 69) says, "the special conditions necessary for silicate rocks to deform in this way seem to be so extrem, especially quartzites, that it is unlikely to occur other than locally in the crust. It seems likely that under physical conditions where metamorphism is possible rocks deform by metamorphic processes as a result of non-hydrostatic pressure. Diffusion is common to all these processes and controls the rates at which they operate. The rocks deform because the shapes of the individual grains are changed by diffusion of atoms and allow the grains to slide over one another. At the same time, as a result of diffusion, nucleation can occur, and grain-boundary migration leads to grain growth and dissolution and change of shape of grains. ..." The present data described and discussed in the preceding pages appears to support FLINN's idea.

The c-axis subfabric of Q_{rg}-grains and that of calcite grains in the specimens I, II and III, and that of Q_{eg}-grains in the specimens V and VI are commonly characterized by a cleft-girdle pattern, with maxima and submaxima on a small circle at 60° to 75° to the girdle axis (=the direction of grain elongation=the L_{1-2}-lineation). It can be pointed out that in the specimens I, II and III the pattern of the c-axis subfabric of quartz is essentially the same as that of calcite, like in the case of deformed calcite-quartz vein described by the senior author (1961). While, in the specimen IV, the c-axis subfabric of Q_{rg}-grains is characterized by a great circle girdle with maxima and submaxima, whose axis coincides with the direction of grain elongation (=the L_{1-2}-lineation), but that of calcite grains is characterized by a small circle

girdle with maxima and submaxima whose angular radius is ca. 60° and whose axis coincides with the direction of grain elongation (=the L_{1-2}-lineation). The latter has the same property as the c-axis subfabric of calcite grains in the other specimens. It can be said on the basis of experimental evidence that the pattern of calcite c-axis subfabrics in question is consistent with axially symmetric extension parallel to the axis of minimal principal stress which coincides with the girdle axis (cf., TURNER *et al.*, 1963). Now, relationship between above-described two types of quartz c-axis subfabric and the stress-strain picture for the calcite c-axis subfabric comes into question. On the basis of correlation between the calcite fabrics and quartz fabrics in a calcite-quartz vein deformed naturally by axial compression, the senior author (1961 and 1963) pointed out that in the metamorphic deformation of quartz aggregate, generally, c-axis of quartz may stably be oriented at an angle ca. 30° to the greatest contraction axis in the system concerned and at an angle ca. 60° to the greatest extension axis, this relation causing the concentration of c-axes in a plane contaning the former and the latter axis. According to this assumption, in the specimens I, II and III the stress-strain picture for the c-axis subfabric of Q_{rg}-grains is consistent with that for calcite c-axis subfabric, while in the specimen IV the former is not consistent with the latter. In order to understand kinematically the two types of quartz c-axis fabric (great-cirle girdle, and small-circle girdle with angular radius of ca. 60°) in question, which are most frequently found in metamorphic tectonites, therefore, further work on the more favourable specimens is required.

Table 1 Summary of dimensional orientation data for the specimens I and V

Nos. of Specimen	Minerals	Sections	Vector Azimuth (degrees)	Vector Magnitude (per cent)	Probability	Significant
V (psammitic matrix)	Q_{ec}-quartz	ac	$\overset{V_{\wedge}S_1}{5}$	55.2	$<10^{-5}$	Yes
		bc	$\overset{V_{\wedge}S_1}{3}$	51.6	$<10^{-5}$	Yes
		ab	$\overset{V_{\wedge}L_{1-2}}{2}$	3.3	>0.90	No
	Q_{eg}-quartz	ac	$\overset{V_{\wedge}S_1}{7}$	68.5	$<10^{-10}$	Yes
		bc	$\overset{V_{\wedge}S_1}{3}$	75.4	$<10^{-10}$	Yes
		ab	$\overset{V_{\wedge}L_{1-2}}{3}$	66.8	$<10^{-5}$	Yes
I (rhyolite pebble)	Q_{rc}-quartz	ac	$\overset{V_{\wedge}S_1}{18}$	23.0	>0.05	No
		bc	$\overset{V_{\wedge}S_1}{24}$	23.0	>0.05	No
		ab	$\overset{V_{\wedge}L_{1-2}}{65}$	17.6	>0.10	No
	Q_{rg}-quartz	ac	$\overset{V_{\wedge}S_1}{8}$	49.1	$<10^{-5}$	Yes
		bc	$\overset{V_{\wedge}S_1}{4}$	48.7	$<10^{-5}$	Yes
		ab	$\overset{V_{\wedge}L_{1-2}}{8}$	29.2	<0.02	Yes
	Calcite	ac	$\overset{V_{\wedge}S_1}{12}$	49.2	$<10^{-5}$	Yes
		ab	$\overset{V_{\wedge}L_{1-2}}{2}$	56.3	$<10^{-5}$	Yes
I (quartz vein)	Q_{vr}-quartz	ac	$\overset{V_{\wedge}S_1}{76}$	42.8	$<10^{-3}$	Yes
		bc	$\overset{V_{\wedge}S_1}{89}$	37.3	$<10^{-3}$	Yes
		ab	$\overset{V_{\wedge}L_{1-2}}{4}$	78.1	$<10^{-10}$	Yes

V: Vector mean

Table 2 Summary of dimensional orientation data for the specimen II

No of Specimen	Minerals	Sections	Vector Azimuth (degrees)	Vector Magnitude (per cent)	Probability	Significant
II (rhyolite pebble)	Q_{rc}-quartz	ac	$V\angle S_1$ 17	17.4	>0.20	No
		bc	$V\angle S_1$ 7	13.1	>0.50	No
		ab	$V\angle L_{1-2}$ 9	22.3	>0.05	No
	Q_{rg}-quartz	ac	$V\angle S_1$ 4	49.1	$<10^{-5}$	Yes
		bc	$V\angle S_1$ 2	51.7	$<10^{-5}$	Yes
		ab	$V\angle L_{1-2}$ 7	85.3	$<10^{-15}$	Yes
	Calcite	ac	$V\angle S_1$ 13	54.5	$<10^{-5}$	Yes

V: Vector mean

Table 3 Summary of dimensional orientation data for the specimen III

No of specimen	Minerals	Sections	Vector Azimuth (degrees)	Vector Magnitude (per cent)	Probability	Significant
III (rhyolite pebble)	Q_{rc}-quartz	ac	$V\angle S_1$ 43	12.3	>0.50	No
		bc	$V\angle S_1$ 7	44.5	$<10^{-4}$	Yes
		ab	$V\angle L_{1-2}$ 32	36.7	<0.01	Yes
	Q_{rg}-quartz	ac	$V\angle S_1$ 19	35.0	<0.01	Yes
		bc	$V\angle S_1$ 10	73.7	$<10^{-10}$	Yes
		ab	$V\angle L_{1-2}$ 8	35.4	<0.01	Yes
	Calcite	ac	$V\angle S_1$ 4	42.9	$<10^{-3}$	Yes
		bc	$V\angle S_1$ 4	73.3	$<10^{-10}$	Yes

V: vector mean

Table 4 Summary of dimensional orientation data for the specimens IV and VI

Nos. of specimen	Minerals	Sections	Vector Azimuth (degrees)	Vector Magnitude (per cent)	Probabitity	Significant
VI (psammitic matrix)	Q_{sc}-quartz	ac	$\overset{V.S_1}{5}$	42.4	$<10^{-3}$	Yes
		bc	$\overset{V.S_1}{1}$	33.0	<0.01	Yes
		ab	$\overset{V.L_{1-2}}{47}$	19.0	>0.10	No
	Q_{sg}-quartz	ac	$\overset{V.S_1}{11}$	29.5	<0.02	Yes
		bc	$\overset{V.S_1}{4}$	42.1	$<10^{-3}$	Yes
		ab	$\overset{V.L_{1-2}}{6}$	79.9	$<10^{-10}$	Yes
IV (rhyolite pebble)	Q_{rc}-quartz	ac	$\overset{V.S_1}{2}$	16.5	>0.20	No
		bc	$\overset{V.S_1}{3}$	9.3	>0.60	No
		ab	$\overset{V.L_{1-2}}{56}$	20.2	>0.10	No
	Q_{rg}-quartz	ac	$\overset{V.S_1}{1}$	55.7	$<10^{-5}$	Yes
		bc	$\overset{V.S_1}{5}$	52.6	$<10^{-5}$	Yes
		ab	$\overset{V.L_{1-2}}{14}$	41.7	$<10^{-3}$	Yes
	Calcite	ac	$\overset{V.S_1}{3}$	38.2	$<10^{-3}$	Yes
		bc	$\overset{V.S_1}{4}$	28.2	<0.02	Yes
		ab	$\overset{V.L_{1-2}}{1}$	28.6	<0.02	Yes

V: Vector mean

Table 5 Summary of dimensional orientation data for Q_{rs}-quartz grains which show the mode of occurrence of the first type, as measured on the ac-section.

Nos. of text-Figs.	Vector Azimuth V-S_1 (degrees)	Vector Azimuth V-B (degrees)	Vector Magnitude (per cent)	Probability	Significant
17			23.0	>0.05	No
18	8	55	26.0	<0.04	Yes
19	81	32	58.5	$<10^{-5}$	Yes
20	13	67	41.1	$<10^{-4}$	Yes
21			20.0	>0.10	No
22			12.8	>0.50	No
23	16	45	41.1	$<10^{-3}$	Yes
24	21	51	49.3	$<10^{-5}$	Yes
25			22.6	>0.10	No
26			16.5	>0.20	No
27	5	53	53.7	$<10^{-5}$	Yes
28	90	57	41.8	$<10^{-3}$	Yes
29			22.8	>0.06	No
30	9	28	30.4	<0.02	Yes

V: Vector mean B: Trend of band consisting of Q_{rs}-grains on the ac-section

Table 6 Summary of dimensional orientation data for Q_{sf}-quartz grains as measured on the ab-section.

Nos. of text-Figs.	Vector Azimuth V-F (degrees)	Vector Magnitude (per cent)	Probability	Significant
44	80	89.4	$<10^{-15}$	Yes
45	72	58.4	$<10^{-5}$	Yes
46	47	96.7	$<10^{-15}$	Yes
47	88	79.5	$<10^{-10}$	Yes

V: Vector mean F: Trend of controlling quartz face on the ab-section

REFERENCES

BARRETT, C.S.B. (1952): *Structure of metals.* McGraw-Hill. New York

BAILEY, S.W., BELL, R.A. and PENG, C.J. (1958): Plastic deformation of quartz in nature. *Geol. Soc. Am. Bull.*, **69**, 1443-1460.

BRACE, W.F. (1955): Quartzite pebble deformation in Central Vermont. *Am. Jour. Sci.*, **253**, 129-145.

_____ (1960): Orientation of anisotropic minerals in a stress field: Discussion. *Geol. Soc. Am. Mem.*, **79**, 9-20.

CAHN, R.W. (1950): Internal strains and recrystallization. *Prog. Metal Physics*, **2**, 151-176.

CARTER, N.L., CHRISTIE, J.M. and GRIGGS, D.T. (1964): Experimental deformation and recrystallization of quartz. *Jour. Geol.*, **72**, 687-733.

CHRISTIE, J.M., GRIGGS, D.T. and GARTER, N.L. (1964): Experimental evidence of basal slip in quartz. *Jour. Geol.*, **72**, 734-756.

CHRISTIE, J.M., and GREEN, H.W. (1964): Several new slip mechanisms in quartz. *Am. Geophys. Union Trans.*, **45**, 103.

CLOOS, E. (1947): Öolite deformation in the South Mountain-fold, Maryland. *Geol. Soc. Am. Bull.*, **58**, 843-918.

CURRAY, J.R. (1956): The analysis of two-dimensional orientation data. *Jour. Geol.*, **64**, 117-131.

DELITSIN, I.S. (1962): The optical orientation of an artificial quartz tectonite. *Doklady, Akad. Nauk. U.S.S.R.*, **146**, 901-904.

DORN, J.E. (1961): *Mechanical behaviour of materials at elevated temperatures.* McGraw-Hill. New York.

FAIRBAIRN, H.W. (1949): *Structural petrology of deformed rocks.* Addison-Wesley Press.

_____ (1950): Synthetic quartzite. *Am. Min.*, **35**, 735-748.

FERREIRA, M.P. and TURNER, F.J. (1964): Microscopic structure and fabric of Yule marble experimentally deformed at different starin rates. *Jour. Geol.*, **72**, 861-875.

FISHER, G. (1926): Gefügeregelung und Granittektonik. *Neues Jahrb. Miner.*, **54**, 95-114.

FLINN, D. (1956): On the deformation of the Funzie conglomerate, Fetlar, Shetland. *Jour. Geol.*, **64**, 480-505.

_____ (1965): Deformation in metamorphism. (in *Controls of metamorphism*, eddited by W.S. PITCHER and Glenys W. FLINN). Oliver & Boyd.

GALWEY, A.K. and JONES, K.A. (1963): An attempt to determine the mechanism of a natural mineral-forming reaction from examination of the products. *Jour. Chem. Soc.* 5681-5686.

GRIGGS, D.T., PATERSON, M.S., HEARD, H.C. and TURNER, F.J. (1960): Annealing recrystallization in calcite crystals and aggregates. *Geol. Soc. Am. Mem.*, **79**, 21-37.

GRIGGS, D.T., TURNER, F.J. and HEARD, H.C. (1960): Deformation of rocks at 500° to 800° C. *Geol. Soc. Am. Mem.*, **79**, 39-104.

GRIGGS, D.T. and BLACIC, J.D. (1964): The strength of quartz in the ductile regime (abstract). *Am. Geophys. Union Trans.*, **45**, 102.

_____ and _____ (1965): Quartz, anomolous weakness of synthetic crystals. *Science*, **147**, 292-295.

HARA, I. (1961): Dynamic interpretation of the simple type of calcite and quartz fabrics in the naturally deformed calcite-quartz vein. *Jour. Sci. Hiroshima Univ. Series* c, **4**, 35-53.

_____ (1963): Revised interpretation of quartz c-axis fabric in metamorphic tectonites (abstract in Japanese). *Jour. Geol. Soc. Japan*, **69**, 322.

_____ (1966a, in press): Dimensional fabric of quartz in a concentric fold. *Jap. Jour. Geol. Geogr.*

_____ (1966b, in press): Strain and movement pictures in competent layers in flexural folding

_____ Deformation of heterogeneously layered rocks in flexural folding (II). *Jour. Geol. Soc. Japan.*

HEARD, H.C. (1963): Effect of large changes in strain rate in the experimental deformation of Yule marble. *Jour. Geol.*, **71**. 162-195.

HERITSCH, H. and PAULITSCH, P. (1954): Über einen Schriftgranit von Radegund bei Graz. *Tschermaks Min. Petrog. Mitt.*, F. 3, Bd. IV, 18-27.

IWASAKI, M. (1963): Metamorphic rocks of the Kōtsu-Bizan area, Eastern Sikoku. *Jour. Facult. Sci. Univ. Tokyo Sec.* II, **15**, Part 1, 1-90.

KAMB, W.B. (1959): Theory of preferred crystal orientation developed by crystallization under stress. *Jour. Geol.*, **67**, 153-170.

_____ (1961): The thermodynamic theory of nonhydrostatically stressed solids. *Jour. Geophys. Res.* **66**, 259-271.

KINGERY, W.D. (1960): *Introduction to Ceramics.* John Wiley & Sons.

KNILL, J.L. (1960): A classification of cleavages, with special references to the Graignish district of the Scotish Highlands. *Inter, Geol. Congress 21st Session*, **18**, 317-325.

KNOPF, E.B. and INGERSON, E. (1938): Structural Petrology. *Geol. Soc. Am. Mem.*, **6**.

KOJIMA, G. (1951): Stratigraphy and geological structure of the crystalline schist region in Central Shikoku (in Japanese, with English abstract). *Jour. Geol. Soc. Japan*, **57**, 177-190.

_____ (1958): The Sambagawa metamorphic zone. *Jubilee Publication on commemoration of 60th birthday of Prof. Jun Suzuki.* (in Japanese), 88-100.

KOJIMA, G. and MITSUNO, C. (1950): On the clastic minerals in the Oboke sandstone schist beds of Yoshinogawa region, Shikoku (in Japanese, with English abstract). *Jour. Geol. Soc. Japan*, **56**, 361-367.

_____ (1966): Geological map of Kawaguchi, Tokushima Prefecture, with an explanatory text (in Japanese). *Geol. Surv. Japan.*

KOJIMA, G., HIDE, K., and YOSHINO, G. (1956): The stratigraphical position of Kieslager in the Sambagawa crystalline schist zone in Shikoku (in Japanese, with English abstract). *Jour. Geol. Soc. Japan*, **62**, 30-45.

KOJIMA, G. and HIDE, K. (1958): Kinematic interpretation of the quartz fabric of triclinic tectonites from Besshi, Central Shikoku, Japan. *Jour. Sci. Hiroshima Univ., Series* C, **2**, 173-193.

KUMAZAWA, M. (1963): A fundamental thermodynamic theory on nonhydrostatic field and on the stability of mineral orientation and phase equilibrium. *Jour. Earth Sci. Nagoya Univ.*, **11**, 145-217.

MACDONALD, G.J.F. (1957): Thermodynamics of solids under nonhydrostatic stress with geologic applications. *Am. Jour. Sci.*, **255**, 266-281.

_____ (1960): Orientation of anisotropic minerals in a stress field. *Geol. Soc. Am. Mem.*, **79**, 1-8.

_____ (1961): The thermodynamic theory of nonhydrostatically stressed solids. *Jour. Geophys. Res.*, **66**, 2599.

MCLEAN, D. (1951): Creep processes in coarse-grained aluminium. *Jour. Inst. Metals*, **80**, 507-519.

_____ (1952): Crystal fragmentation in aluminium during creep. *Jour. Inst. Metals*, **81**, 287-292.

MIYASHIRO, A. (1965): *Metamorphic rocks and metamorphic belts.* (in Japanese). Iwanami.

MÜGGE, O. (1928): Über die Entstehung faseriger Minerale und ihrer Aggregationsformen. *Neues Jahrb. Beilb.*, **58** A, 303-348.

NAKAGAWA, M. (1965): Structural petrology of the Oboke Anticline in the Sambagawa crystalline schist zone, Central Shikoku. *Geol. Rep. Hiroshima Univ.*, **14**, 345-368.

NAKAYAMA, I. (1964): The relation of mineral composition to the petrofabrics in the crystalline schists of Eastern Shikoku (in Japanese. with English abstract). *Jour. Geol. Soc. Japan*, **70**, 204-213.

OFTEDAHL, C. (1948): Deformation of quartz conglomerate in Central Norway. *Jour. Geol.*, **56**, 476-487.

PABST, A. (1931): "Pressure-shadows" and the measurement of the orientation of minerals in rocks. *Am. Miner.*, **16**, 55-70.

PATERSON, M.S. and WEISS, L.E. (1961): Symmetry concepts in the structural analysis of deformed rocks. *Geol. Soc. Am. Bull.*, **72**, 841-882.

PAULITSCH, P. and AMBS, H. (1963): Undulation in Quartzgeröllen. *Tschermaks Miner. Petrog. Mitt.*, **8**, 579-590.

RALEIGH, C.B. (1965): Crystallization and recrystallization of quartz in a simple pistoncylinder device. *Jour. Geol.*, **73**, 369-377.

RAMBERG, H. (1952): *The origin of metamorphic and metasomatic rocks.* The University of Chikago Press.

RUTHERFORD, J.J.B., ABORN, R.H. and BAIN, E.C. (1937): Grain area on a plane section and the grain size of a metal. *Metals & Alloys*, **8**, 345-348.

SANDER, B. (1930): *Gefügekunde der Gesteine.* Vienna, Springer verlag.

_____ (1948): *Einführung in dir Gefügekunde der geologischen Körper*, Ier Teil, Wien und Innsbruck.

_____ (1950): *Einführung in die Gefügekunde der geologischen Körper*, IIer Teil, Wien und Innsbruck.

SCHEIL, Von E. (1935): Statistische Gefügeuntersuchungen I. *Metalkunde*, **27**, 199-209.

SCHMIDT, W. (1932): *Tektonik und Verformungslehre.* Borntraeger, Berlin.

TURNER, F.J. and CH'IH. C.S. (1951): Deformation of Yule marble, Part III. *Geol. Soc. Am. Bull.*, **62**, 887-906.

TURNER, F.J., GRIGGS, D.T. and HEARD, H. (1954): Experimental deformation of calcite crystals. *Geol. Soc. Am. Bull.*, **65**, 883-934.

TURNER, F.J., GRIGGS, D.T., CLARK, R.H. and DIXON, R.H. (1956): Deformation of Yule marble, Part VII.. *Geol. Soc. Am. Bull.*, **67**, 1259-1293.

TURNER, F.J. and WEISS, L.E. (1963): *Structural Analysis of metamorphic tectonites.* McGraw Hill. New York.

I. HARA: INSTITUTE OF GEOLOGY AND MINERALOGY, FACULTY OF SCIENCE, HIROSHIMA UNIVERSITY.

Y. NISHIMURA: INSTITUTE OF GEOLOGY AND MINERALOGY, FACULTY OF SCIENCE, HIROSHIMA UNIVERSITY.

T. ISAI: INSTITUTE OF GEOLOGY AND MINERALOGY, FACULTY OF SCIENCE, HIROSHIMA UNIVERSITY.

Explanation of Plate VII

Fig. 1 The conglomerate schist (Psammitic matrix and remarkablly elongated rhyolite pebbles).

Fig. 2 Quartz grains (Q_{rg}-grains) in the recrystallized ground-mass of rhyolite pebble (specimen II). Crossed nicols.

FIG. 1

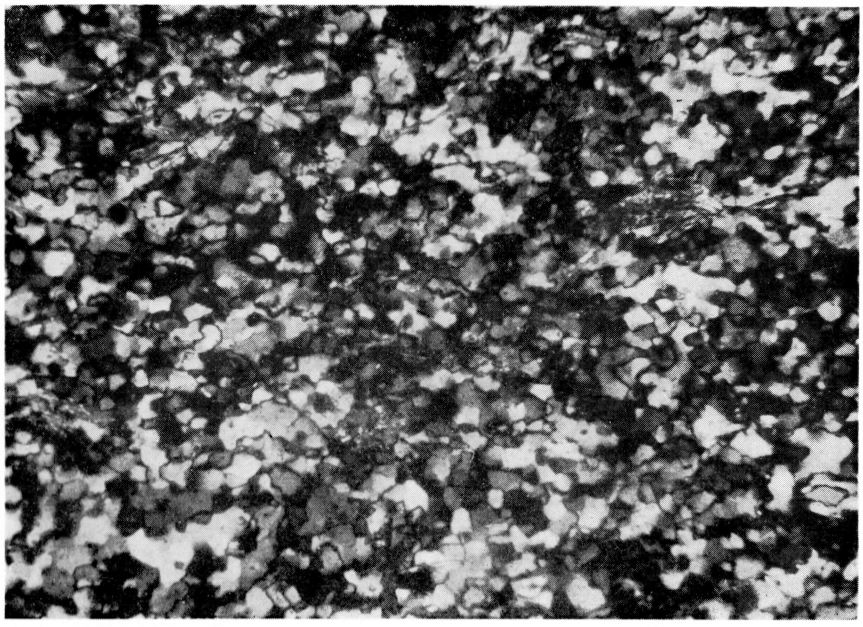

FIG. 2

Explanation of Plate VIII

Fig. 1 Feather quartz (Q_{sf}-grains) and white mica in the pressure-shadow surrounding Q_{sc}-grain in the psammitic schist, observed on the ab-section. Crossed nicols.

Fig. 2 Feather quartz (Q_{rf}-grains) and white mica in the pressure-shadow surrounding Q_{rc}-grain in the rhyolite pebble, observed on the ab-section. Crossed nicols.

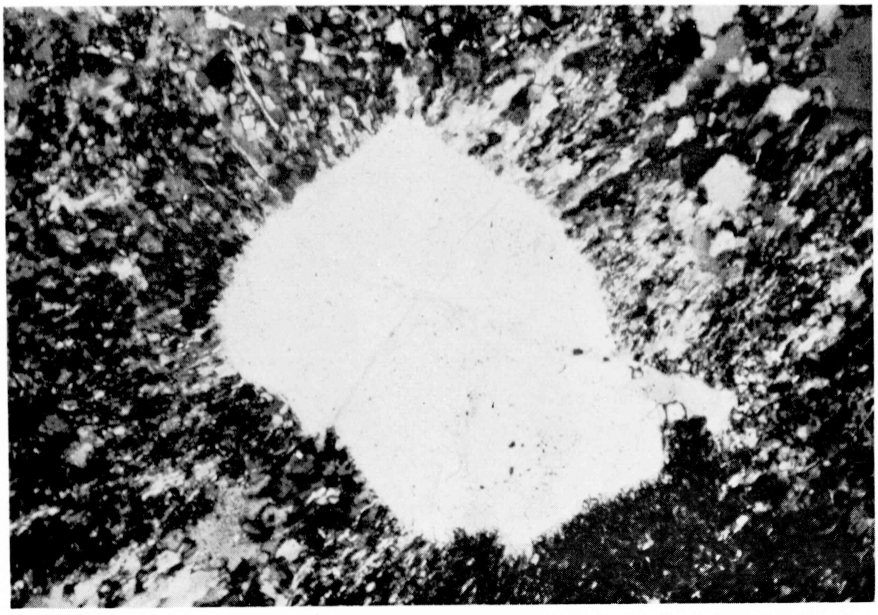

FIG. 1

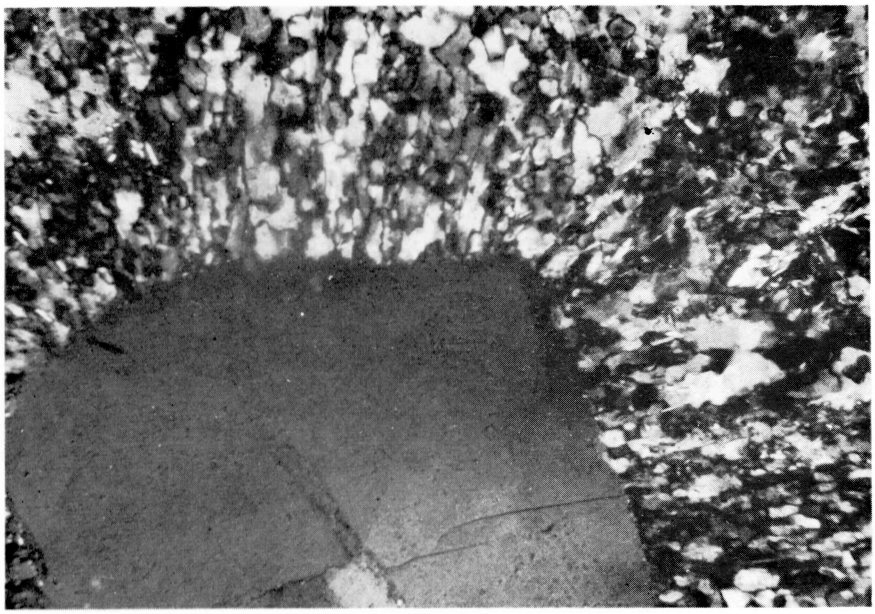

FIG. 2

Explanation of Plate IX

Fig. 1 Q_{rs}-grains which show the mode of occurrence of the first type (band). Crossed nicols.

Fig. 2 Q_{rs}-grains which show the mode of occurrence of the second type. Crossed nicols.

Fig. 3 Q_{vs}-grains in the rhyolite pebble (specimen I). Crossed nicols. X

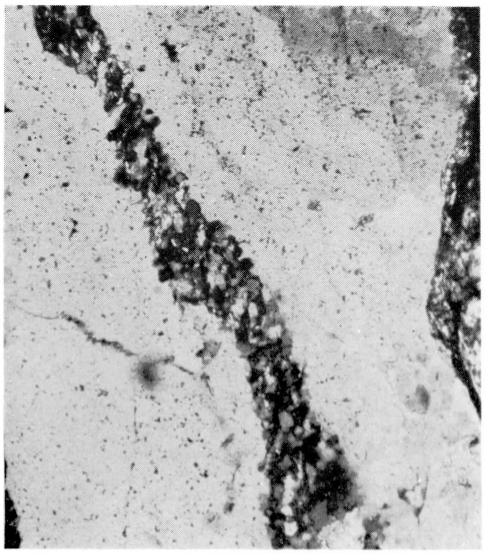

FIG.1

FIG. 2

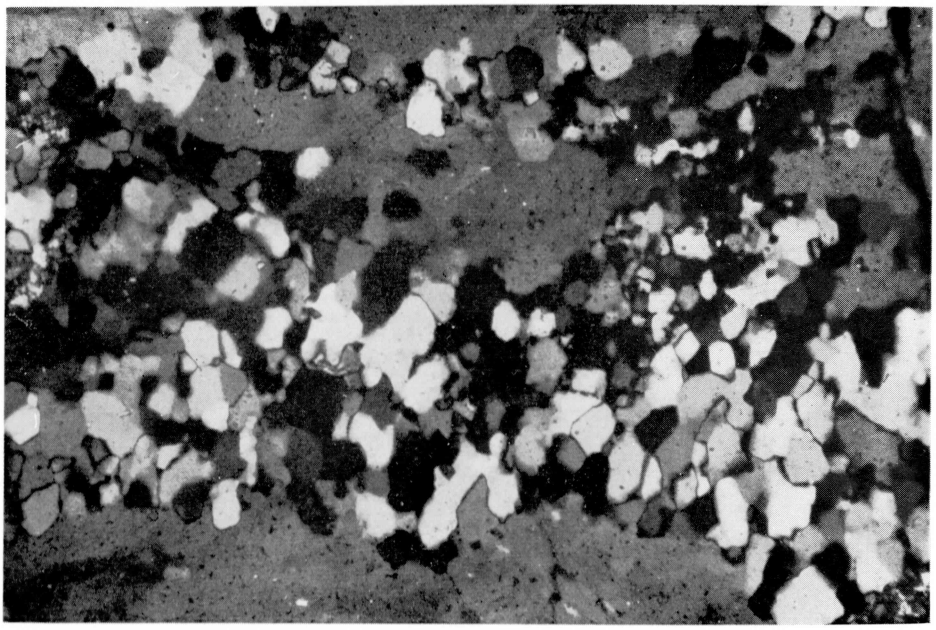

FIG. 3

Explanation of Plate X

Fig. 1 Q_{vs}-grains in the pelitic schist of the Oboke district. Crossed nicols.

Fig. 2 Q_{vs}-grains in the basic schist of the Oboke district. Crossed nicols.

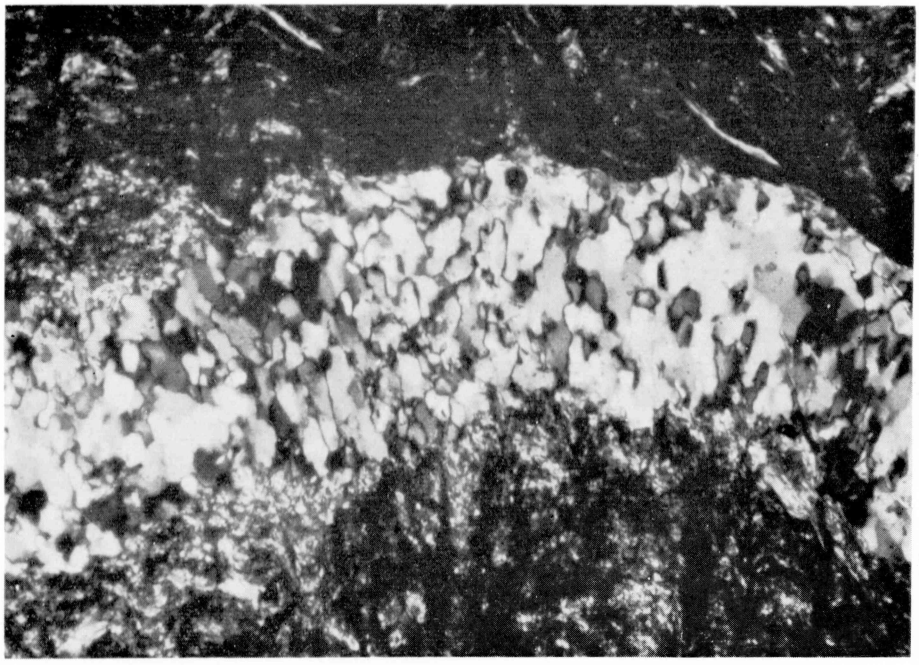

FIG. 1

FIG. 2